Modeling and simulation of the cavitation phenomenon in space engine turbopumps

Joris Cazé

Directeurs de thèse : Fabien Petitpas, Eric Daniel

Référents CNES : Sébastien Le Martelot, Matthieu Queguineur

Summary

Introduction

Modeling of the cavitation phenomenon

- State-of-the-art
- Two-phase flow approach
- Two-phase flow model
- Blades motion

Numerical method

- Numerical scheme
- MRF fluxes
- Mesh mapping

Results

- Test case setup
- Single-phase flow behavior: pump characteristic
- Two-phase flow: cavitating regime

Conclusions & perspectives

Summary

Introduction

Modeling of the cavitation phenomenon

- State-of-the-art
- Two-phase flow approach
- Two-phase flow model
- Blades motion

Numerical method

- Numerical scheme
- MRF fluxes
- Mesh mapping

Results

- Test case setup
- Single-phase flow behavior: pump characteristic
- Two-phase flow: cavitating regime

Conclusions & perspectives

Introduction: overview

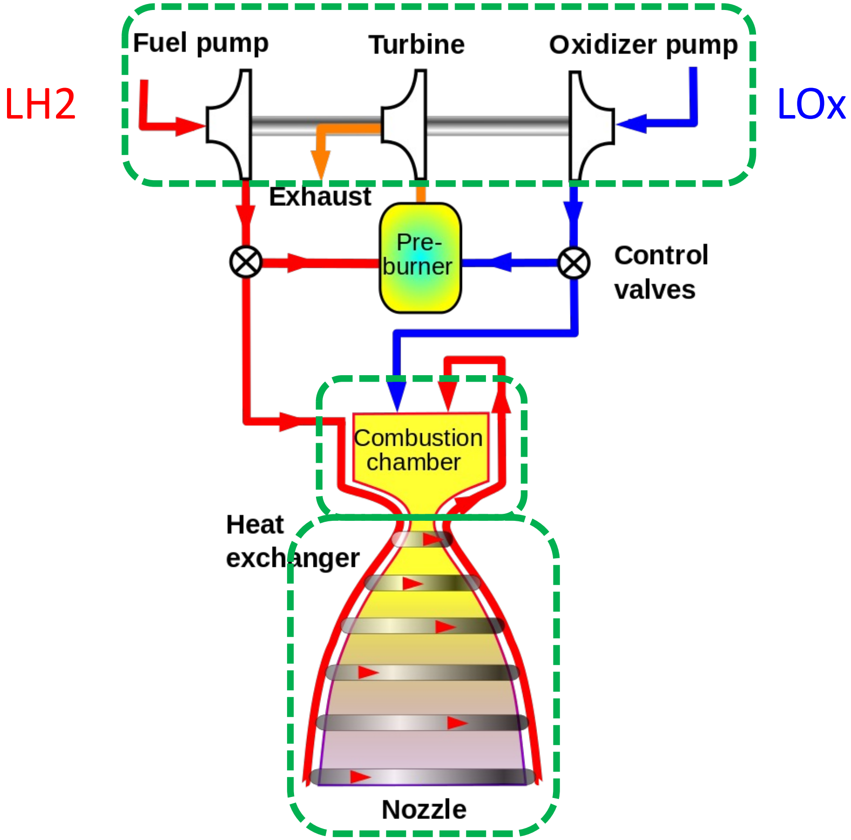

Fig – Vulcain gas generator cycle

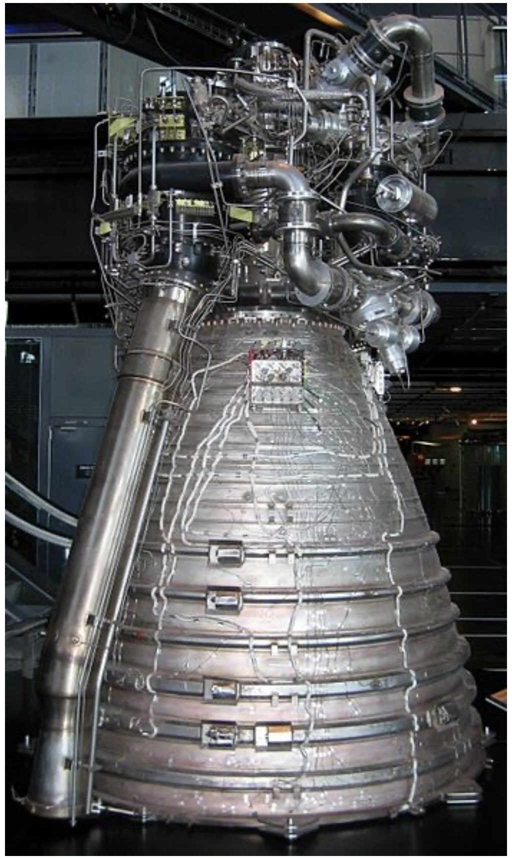

Fig – Vulcain 1 rocket engine

Introduction: turbopump

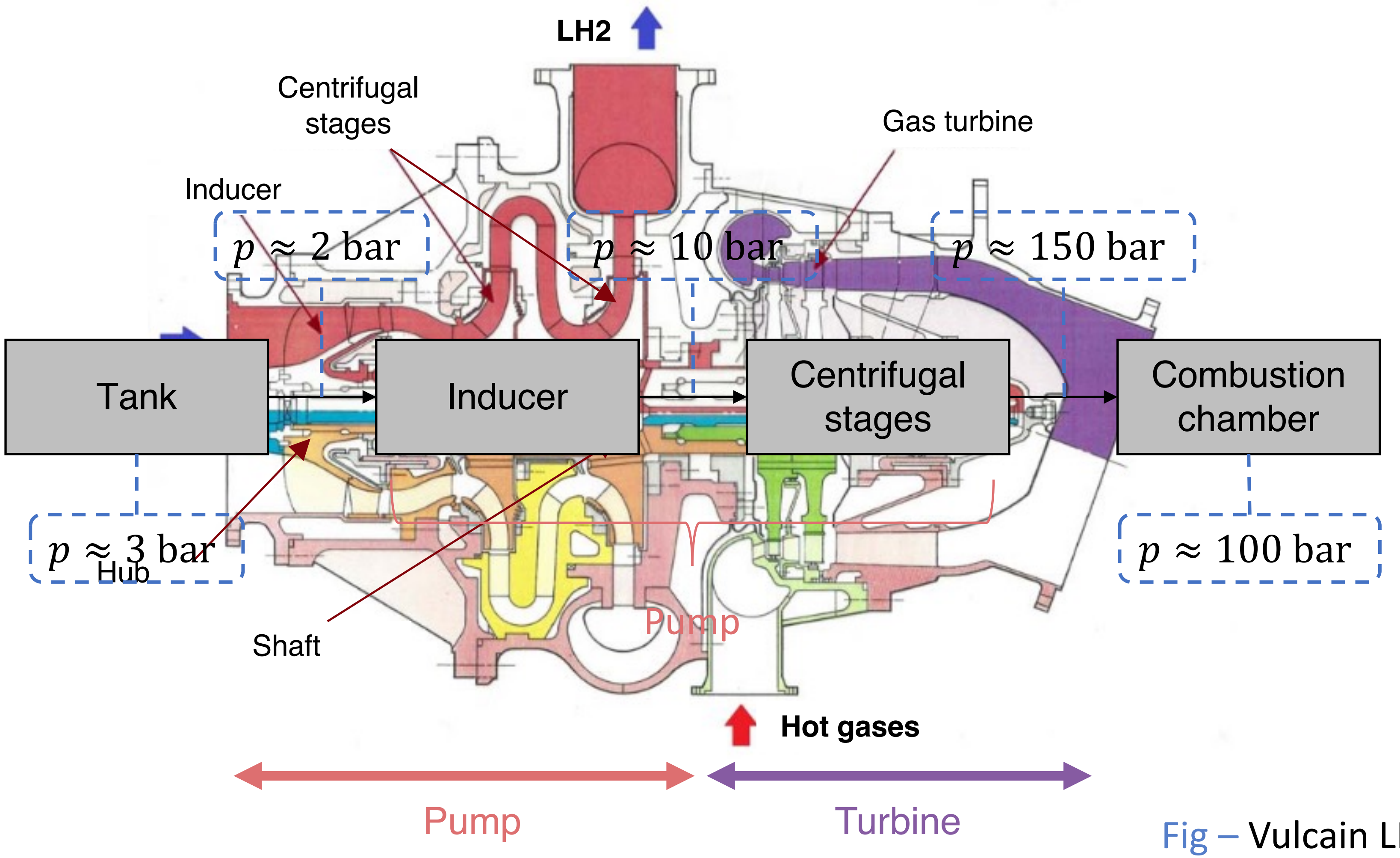

Fig – Vulcain LH2 turbopump

Introduction: cavitation

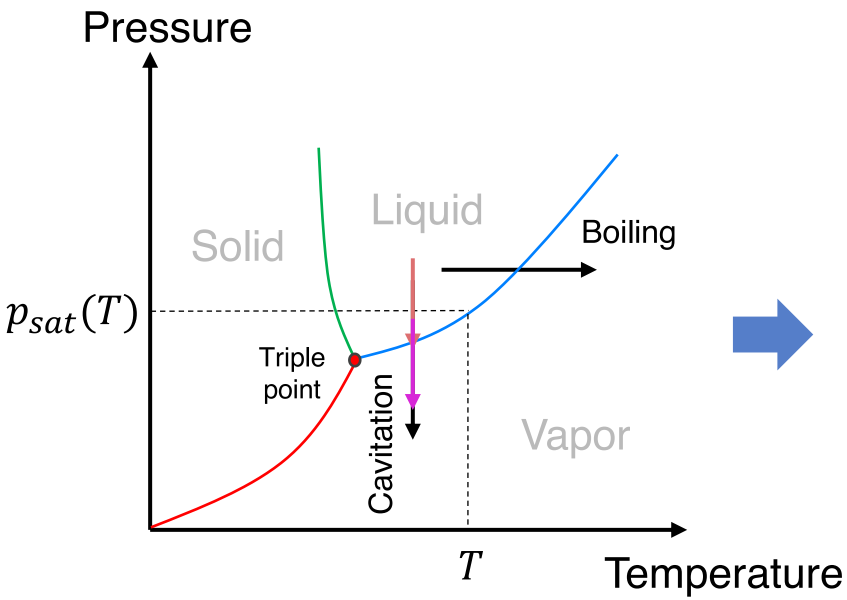

$$p(T) < p_{sat}(T)$$

- Pump suction
- Local overspeed
- Shear stress
- Geometry

No cavitation or moderate cavitation

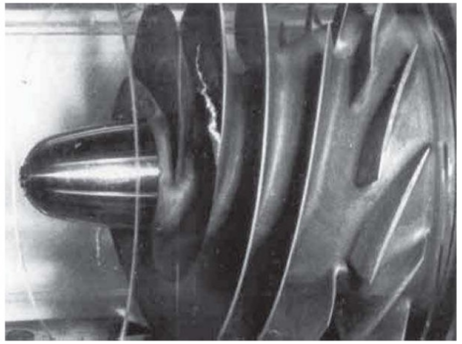

Strong cavitation

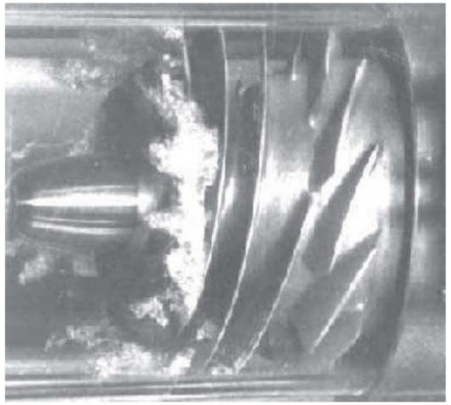

- Mechanical instabilities
- Performance drop

Fig – Cavitation on SSME LOx inducer [Braisted, 1980]

Introduction: objectives

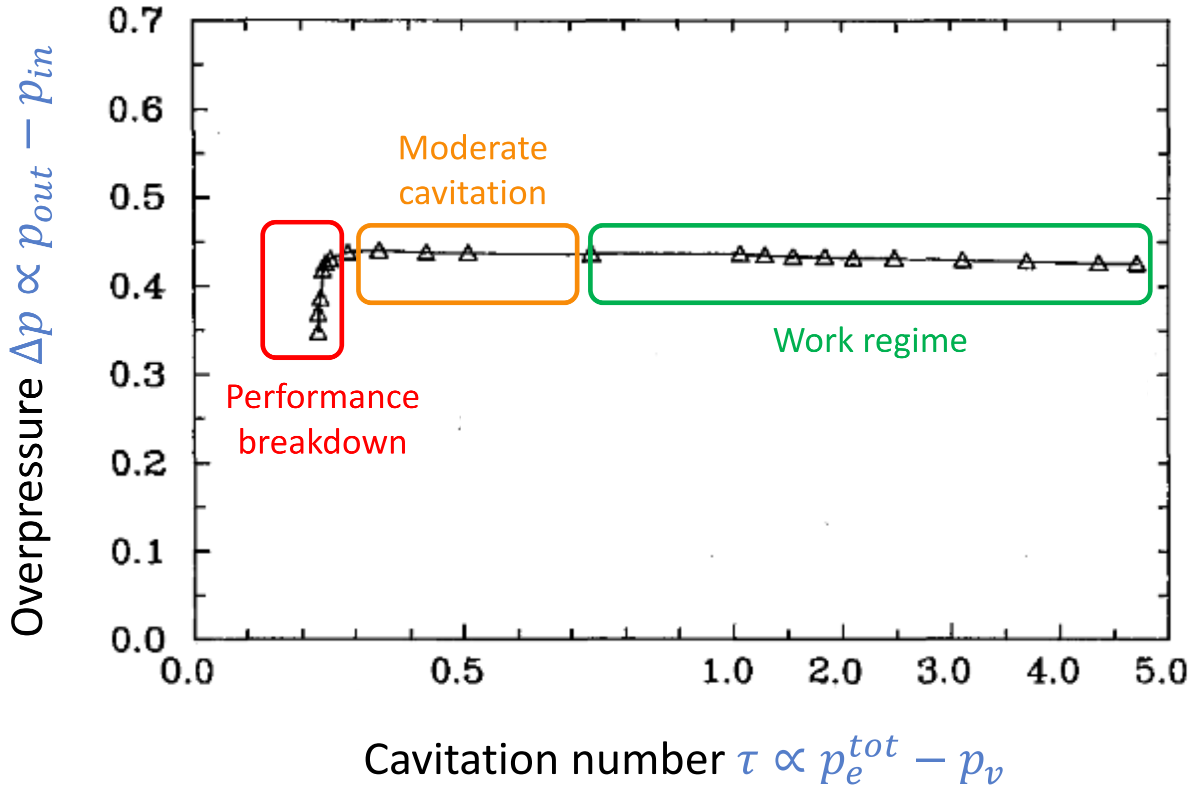

Fig – Experimental performance curve on a centrifugal pump [Franz *et al.*, 1989]

Fig – Illustration of a liquid propellant tank

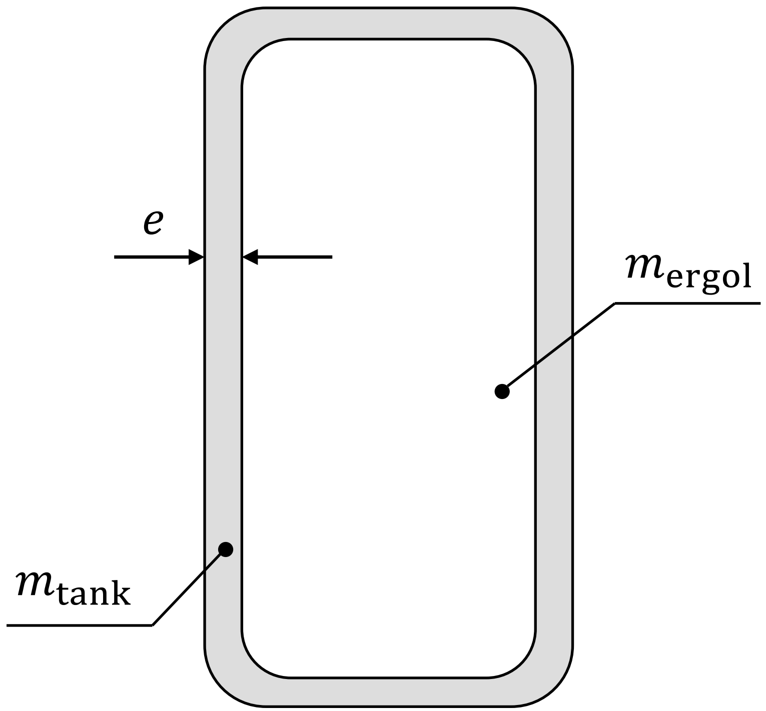

Reduce the rocket dry mass

Introduction: cavitation modeling

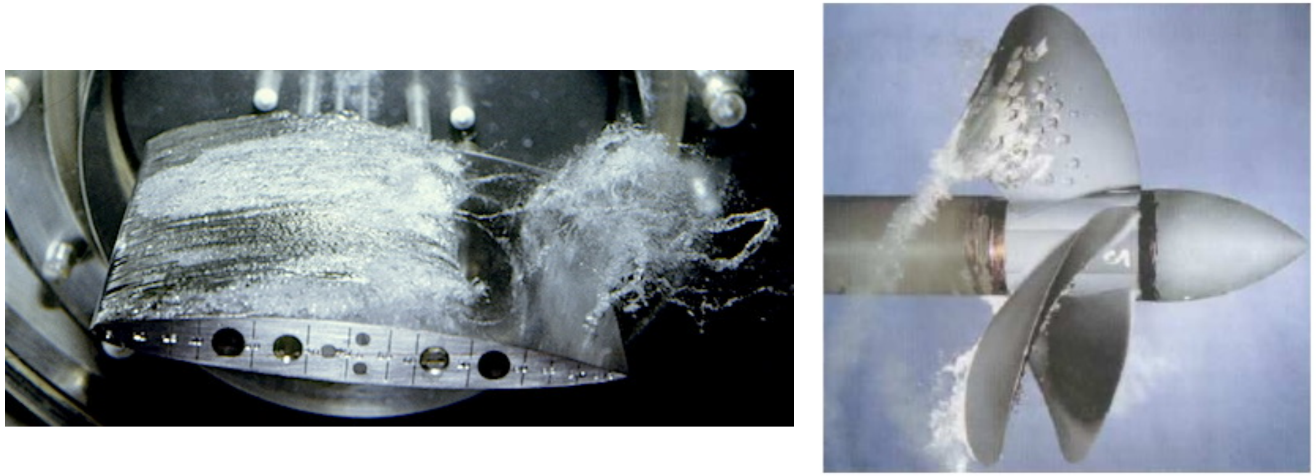

Fig – Cloud cavitation on hydrofoil (left) - Bubble cavitation on propeller (right)
[Franc and Michel, 1995]

Cavitation characteristics:

- Two-phase flow
- Phase change
- (in)compressible regions
- 3D

Pump characteristic:

- Rotor motion

Summary

Introduction

Modeling of the cavitation phenomenon

- State-of-the-art
- Two-phase flow approach
- Two-phase flow model
- Blades motion

Numerical method

- Numerical scheme
- MRF fluxes
- Mesh mapping

Results

- Test case setup
- Single-phase flow behavior: pump characteristic
- Two-phase flow: cavitating regime

Conclusions & perspectives

Modeling: state-of-the-art

Bubble dynamics

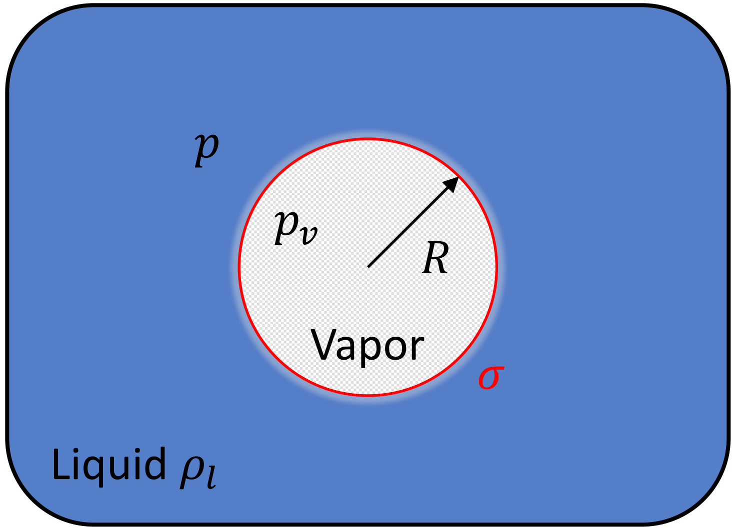

Rayleigh-Plesset equation

$$R\frac{\mathrm{d}^2R}{\mathrm{d}t^2}+\frac{3}{2}\left(\frac{\mathrm{d}R}{\mathrm{d}t}\right)^2+\frac{2\sigma}{R}=\frac{p_v-p}{\rho_l}$$

$$\dot{m}=\pm N4\pi R^2\rho_v\sqrt{\frac{2}{3}\frac{p_v-p}{\rho_l}}$$

Empirical correction coefficients

[Singhal *et al.*, 2002] [Zhang *et al.*, 2019]

Modeling: state-of-the-art

Barotropic EOS

- Homogeneous model
- 3D RANS → FINE™/Turbo code

$$\rho = \alpha_v \rho_v + (1 - \alpha_v)\rho_l$$

$$\frac{\partial \rho}{\partial t} + \nabla \cdot (\rho \boldsymbol{u}) = 0$$

$$\frac{\partial \rho \boldsymbol{u}}{\partial t} + \nabla \cdot (\rho \boldsymbol{u} \otimes \boldsymbol{u} + p\boldsymbol{I}) = \nabla \cdot \boldsymbol{\tau} + \rho \boldsymbol{F}$$

$$\rho = \rho(p) = \frac{\rho_l + \rho_v}{2} + \frac{\rho_l - \rho_v}{2} \sin\left(\frac{p - p_v}{c_{min}^2} \frac{2}{\rho_l - \rho_v}\right)$$

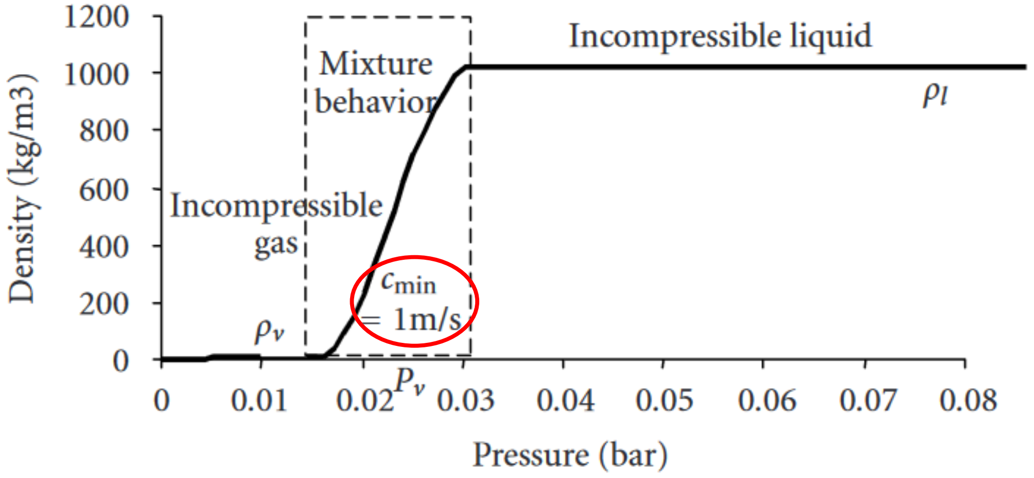

Fig - Barotropic state law $\rho(p)$ for water from [Coutier-Delgosha *et al.*, 2005]

- No need to define mass transfer
- Better thermodynamic behavior with the added energy equation [Goncalves *et al.*, 2010]

Modeling: two-phase flow approach

- Hyperbolic model → waves propagation
- Able to handle several interface types L/V or others (multi-species, non-condensable gases)

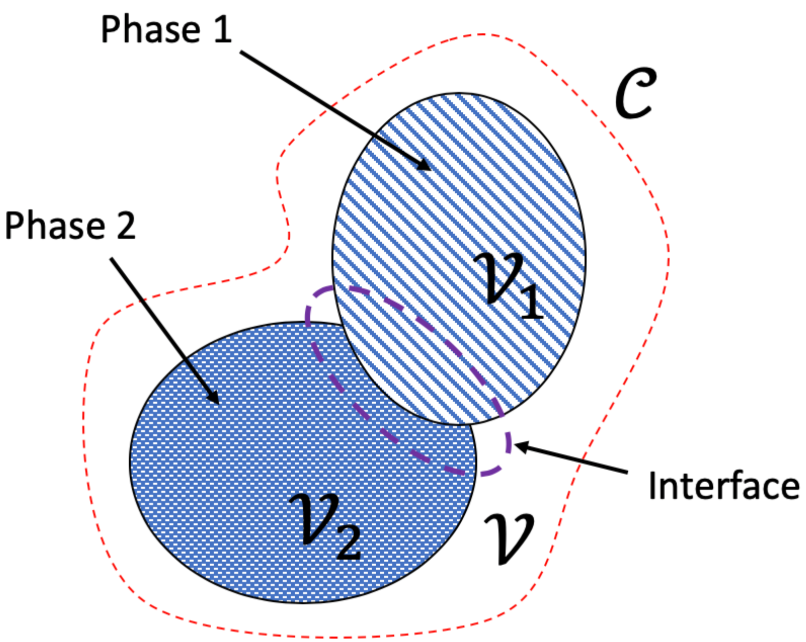

- Complete thermodynamic description for each phase
- Taking into account the thermodynamic equilibrium

} Phase change

Modeling: two-phase flow model

Velocity equilibrium model ($\boldsymbol{u}_1 = \boldsymbol{u}_2$)

Used to study cavitating flow [Petitpas *et al.*, 2011]

For two-phase flow $k = 1, 2$:

$$\partial_t \alpha_1 + \nabla \cdot (\alpha_1 u) - \alpha_1 \nabla \cdot u = \mu(p_1 - p_2) + \boxed{\dot{m}/\rho_I}$$

$\nu(g_2 - g_1)/\rho_I$

$$\partial_t(\alpha_k \rho_k) + \nabla \cdot (\alpha_k \rho_k \boldsymbol{u}) = \pm_k \boxed{\dot{m}}$$

$\nu(g_2 - g_1)$

$$\partial_t(\rho \boldsymbol{u}) + \nabla \cdot (\rho \boldsymbol{u} \otimes \boldsymbol{u}) + \nabla(\alpha_1 p_1 + \alpha_2 p_2) = \boldsymbol{0}$$

$\nu(g_2 - g_1)$

$$\partial_t(\alpha_k \rho_k e_k) + \nabla \cdot (\alpha_k \rho_k e_k \boldsymbol{u}) + \alpha_k p_k \nabla \cdot \boldsymbol{u} = \mp_k \mu p_I (p_1 - p_2) \pm_k h_I \boxed{\dot{m}} \pm_k \boxed{\dot{Q}}$$

$\theta(T_2 - T_1)$

$$\Downarrow$$

$$\partial_t U + \nabla \cdot F(U) + H(U) \nabla \cdot u = R(U)$$

+

EOS
$e_k = e_k(\rho_k, p_k)$

[Kapila *et al.*, 2000]
[Saurel *et al.*, 2009]

Modeling: thermodynamical closure

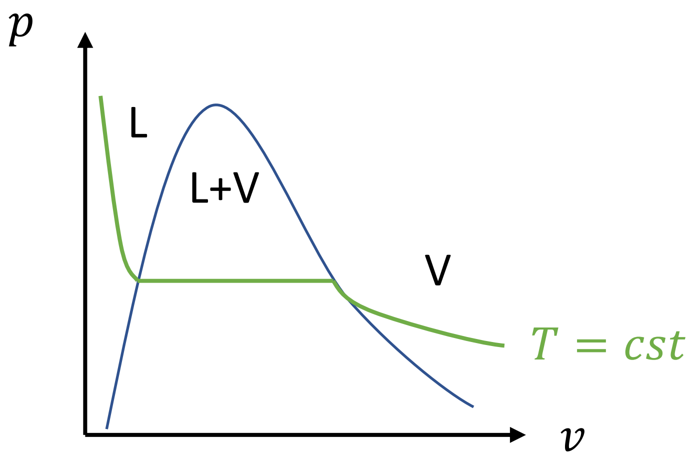

Fig – Typical phase diagram (p, v)

- Each phase is governed by its Equation Of State (EOS)
- EOS
  - Stiffened Gas
  - Noble-Abel Stiffened Gas

$\neq$ Van Der Waals

- Calibration of EOS parameters based on experimental saturation curve
  [Le Métayer *et al.*, 2004]
  [Le Métayer *et al.*, 2016]

Thermal agitation

Matter cohesion

$$p(v,e) = (\gamma - 1)\frac{e-q}{v-b} - \gamma p_\infty$$

Repulsive short distance effects

Modeling: thermodynamical closure

<u>Example</u> Water EOS calibration for

- Stiffened Gas
- Noble-Abel Stiffened Gas

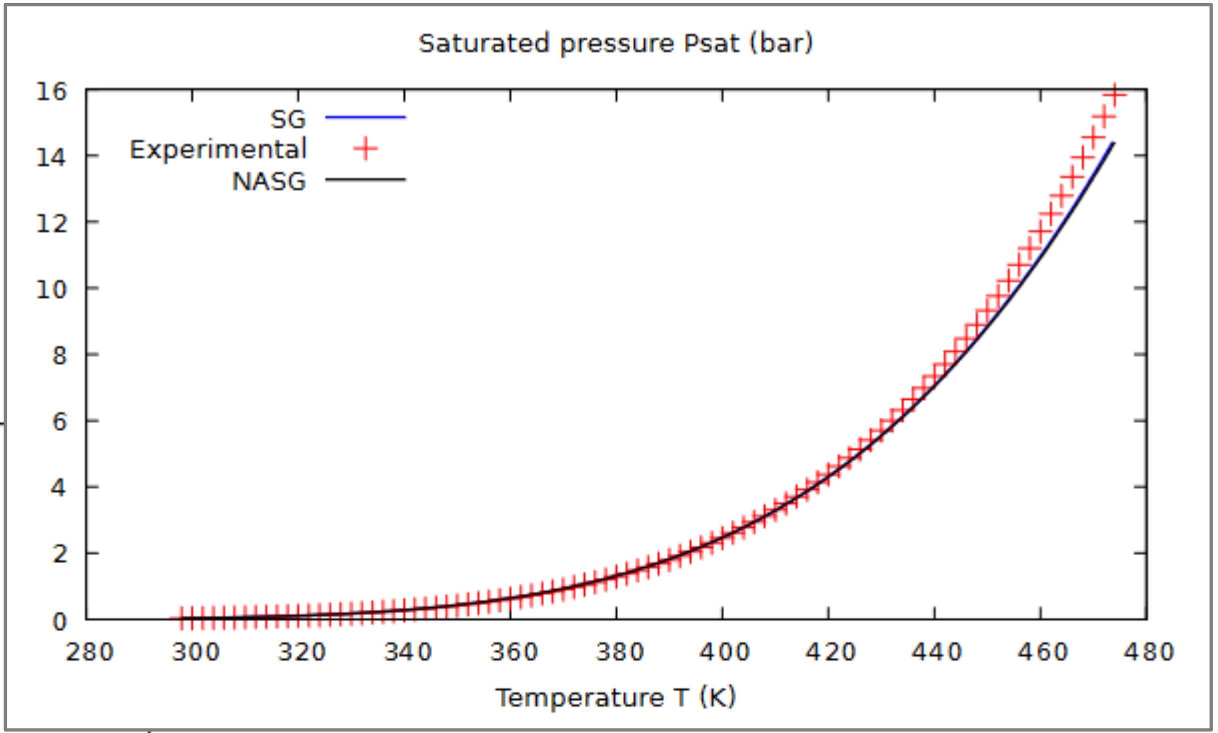

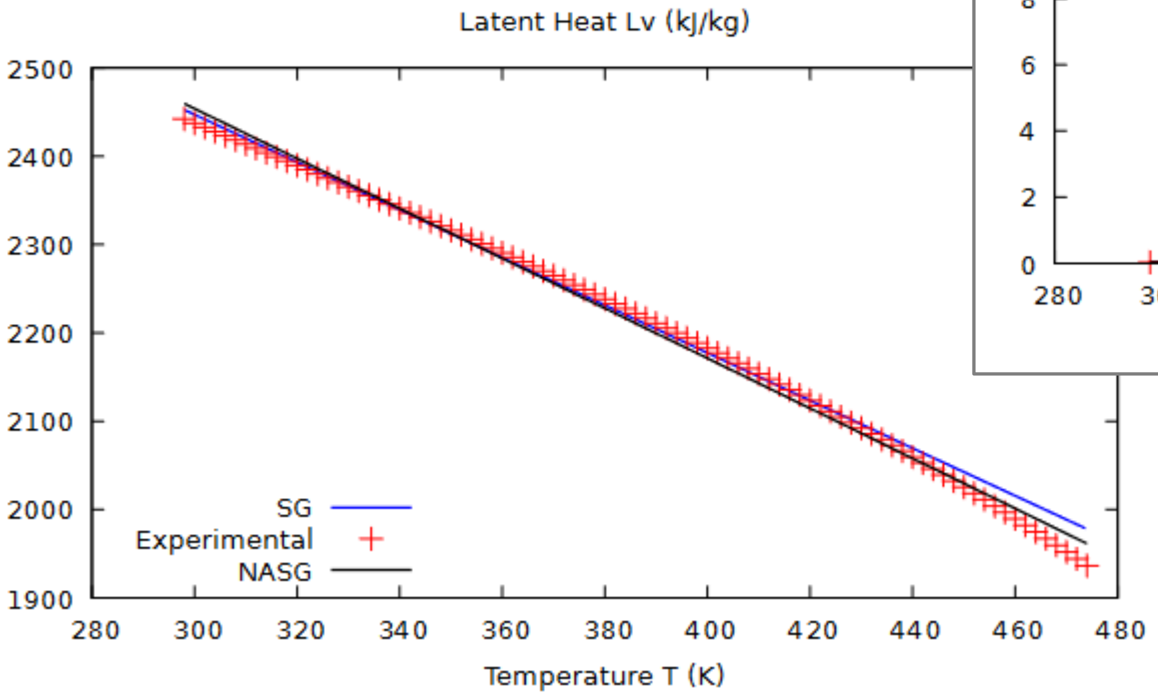

Fluid state is solely based on thermodynamic considerations

Modeling: blades motion

Moving Reference Frame (MRF) method [Combrinck and Dala, 2014]

Lagrangian derivation based on classical point mechanics

Change of reference frame: inertial one → rotating one

Rotationnal effects: centrifugal force & Coriolis force

Euler equations:

$$\partial_t \rho + \nabla \cdot \rho \boldsymbol{u_r} = 0$$

$$\partial_t \rho \boldsymbol{u_r} + \nabla \cdot (\rho \boldsymbol{u_r} \otimes \boldsymbol{u_r} + pI) = -2\,\rho \boldsymbol{\Omega} \wedge \boldsymbol{u_r} - \rho \boldsymbol{\Omega} \wedge (\boldsymbol{\Omega} \wedge \boldsymbol{x})$$

$$\partial_t \rho E_r + \nabla \cdot \big((\rho E_r + p)\boldsymbol{u_r}\big) = -\rho \boldsymbol{u_r} \cdot \big(\boldsymbol{\Omega} \wedge (\boldsymbol{\Omega} \wedge \boldsymbol{x})\big)$$

$$E_r = e + \frac{1}{2}\boldsymbol{u_r^2}$$

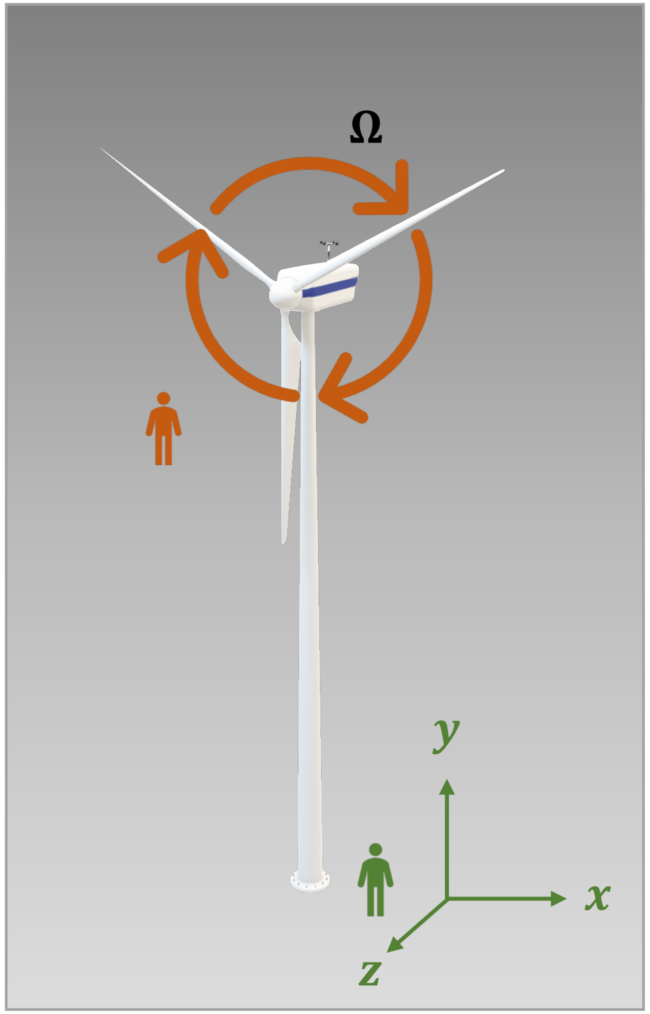

$$\boldsymbol{u} = \boldsymbol{u_r} + \boldsymbol{\Omega} \times \boldsymbol{r}$$

[Cazé *et al.*, 2022]

Modeling: blades motion

Change of reference frame: inertial one → rotating one
Rotationnals effects: centrifugal force & Coriolis force

Two-phase flow model:

$$\partial_t \alpha_1 + \boldsymbol{u_r} \cdot \nabla \alpha_1 = \mu(p_1 - p_2) + \frac{\dot{m}}{\rho_I}$$

$$\partial_t(\alpha_k \rho_k) + \nabla \cdot (\alpha_k \rho_k \boldsymbol{u}) = \pm_k \dot{m}$$

$$\partial_t(\rho \boldsymbol{u_r}) + \nabla \cdot (\rho \boldsymbol{u_r} \otimes \boldsymbol{u_r}) + \nabla(\alpha_1 p_1 + \alpha_2 p_2) = -2\,\rho \boldsymbol{\Omega} \wedge \boldsymbol{u_r} - \rho \boldsymbol{\Omega} \wedge (\boldsymbol{\Omega} \wedge \boldsymbol{x})$$

$$\partial_t(\alpha_k \rho_k e_k) + \nabla \cdot (\alpha_k \rho_k e_k \boldsymbol{u_r}) + \alpha_k p_k \nabla \cdot \boldsymbol{u_r} = \mp_k\, \mu p_I (p_1 - p_2) \pm_k (\dot{Q} + h_I \dot{m})$$

$$\partial_t \rho E_r + \nabla \cdot \big((\rho E_r + p)\boldsymbol{u_r}\big) = -\rho \boldsymbol{u_r} \cdot \big(\boldsymbol{\Omega} \wedge (\boldsymbol{\Omega} \wedge \boldsymbol{x})\big)$$

$$E_r = e + \frac{1}{2}\boldsymbol{u_r^2} \qquad e = Y_1 e_1 + Y_2 e_2$$

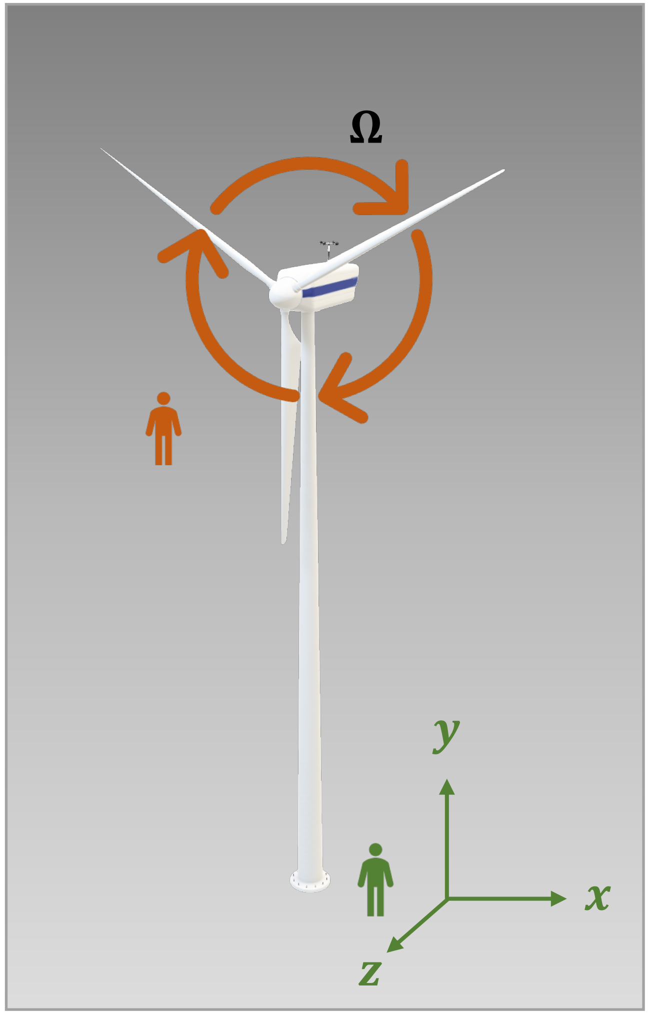

$$\boldsymbol{u} = \boldsymbol{u_r} + \boldsymbol{\Omega} \times \boldsymbol{r}$$

[**Cazé** *et al.*, 2022]

Summary

Introduction

Modeling of the cavitation phenomenon

- State-of-the-art
- Two-phase flow approach
- Two-phase flow model
- Blades motion

Numerical method

- Numerical scheme
- MRF fluxes
- Mesh mapping

Results

- Test case setup
- Single-phase flow behavior: pump characteristic
- Two-phase flow: cavitating regime

Conclusions & perspectives

Numerical method: Overview

Solving $\partial_t U + \nabla \cdot F(U) + \Sigma(U) = R(U) + S(U)$ using FV method:

1. Homogeneous system with Godunov's scheme $\partial_t U + \nabla \cdot F(U) + \Sigma(U) = 0$
2. Source step $\partial_t U = S(U)$
3. Phase change $\partial_t U = R_{pTg}(U)$

[Schmidmayer *et al.*, 2020] & [Schmidmayer, **Cazé** *et al.*, 2022]

Numerical method: numerical scheme

Solving $\partial_t U + \nabla \cdot F(U) + \Sigma(U) = R(U) + S(U)$ using FV method:

1. Homogeneous system with Godunov's scheme $\partial_t U + \nabla \cdot F(U) + \Sigma(U) = 0$

$$\boldsymbol{U}_{\boldsymbol{i}}^{\boldsymbol{n+1}} = \boldsymbol{U}_{\boldsymbol{i}}^{\boldsymbol{n}} - \frac{\Delta t}{V_i}\left(\Sigma_{s=1}^{N_s} A_s \boldsymbol{F}_{\boldsymbol{s}}^{*} \cdot \boldsymbol{n}_{\boldsymbol{s}}\right) - \frac{\Delta t}{V_i} H(\boldsymbol{U}_{\boldsymbol{i}}^{\boldsymbol{n}})\left(\Sigma_{s=1}^{\mathrm{N_s}} A_s \boldsymbol{u}_{\boldsymbol{s}}^{*} \cdot \boldsymbol{n}_{\boldsymbol{s}}\right)$$

with $\boldsymbol{F}_{\boldsymbol{s}}^{*} = RP(\boldsymbol{U}_{\boldsymbol{i}}^{\boldsymbol{n}}, \boldsymbol{U}_{\boldsymbol{j}}^{\boldsymbol{n}})$ using approximate Riemann solver

Numerical method: numerical scheme

Solving $\partial_t U + \nabla \cdot F(U) + \Sigma(U) = R(U) + S(U)$ using FV method:

1. Homogeneous system with Godunov's scheme $\partial_t U + \nabla \cdot F(U) + \Sigma(U) = 0$
2. Source step $\partial_t U = S(U)$

➡ Take into account Moving Reference Frame terms

$$\boldsymbol{U_i^{n+1}} = \widetilde{\boldsymbol{U_i^n}} + \Delta t\, \boldsymbol{S}(\boldsymbol{U_i^n})$$

or RK2, RK4 scheme

Numerical method: numerical scheme

Solving $\partial_t U + \nabla \cdot F(U) + \Sigma(U) = R(U) + S(U)$ using FV method:

1. Homogeneous system with Godunov's scheme $\partial_t U + \nabla \cdot F(U) + \Sigma(U) = 0$
2. Source step $\partial_t U = S(U)$
3. Phase change $\partial_t U = R_{pTg}(U)$

$$
\begin{aligned}
&\partial_t \alpha_1 = \mu(p_1 - p_2) + \nu(g_2 - g_1)/\rho_I \\
&\partial_t(\alpha_k \rho_k) = \pm_k \nu(g_2 - g_1) \\
&\partial_t(\rho \boldsymbol{u}) = \boldsymbol{0} \\
&\partial_t(\alpha_k \rho_k e_k) = \mp_k \mu p_I(p_1 - p_2) \pm_k h_I \nu(g_2 - g_1) \pm_k \theta(T_2 - T_1)
\end{aligned}
$$

Evaluation of mass transfer terms by relaxation processes

⬇

Thermodynamic problem of return to equilibrium

with $\mu, \nu, \theta \to \infty$

Numerical method: phase change

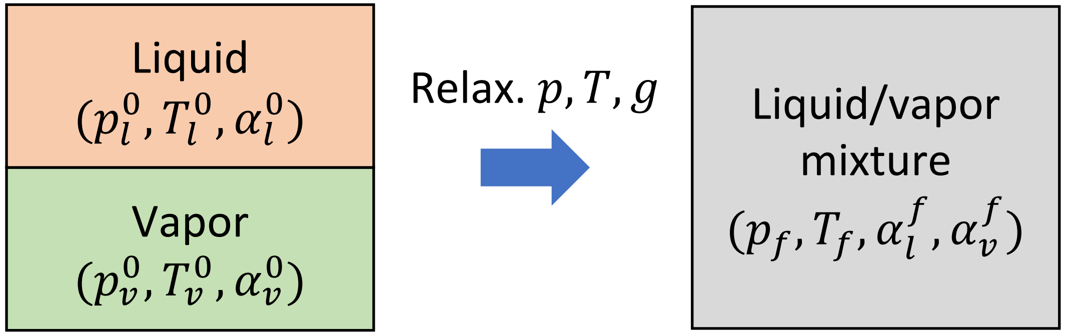

EDO

Saturation state

$$T_l^f = T_v^f = T^f$$
$$p_l^f = p_v^f = p^f$$
$$g_l^f = g_v^f = g^f$$

Mass conservation

$$\rho^f = \alpha_v^f \rho_v^f + \alpha_l^f \rho_l^f = \rho^0 \quad (1)$$

Energy conservation

$$(\rho e)^f = (\alpha \rho e)_v^f + (\alpha \rho e)_l^f = (\rho e)^0 \quad (2)$$

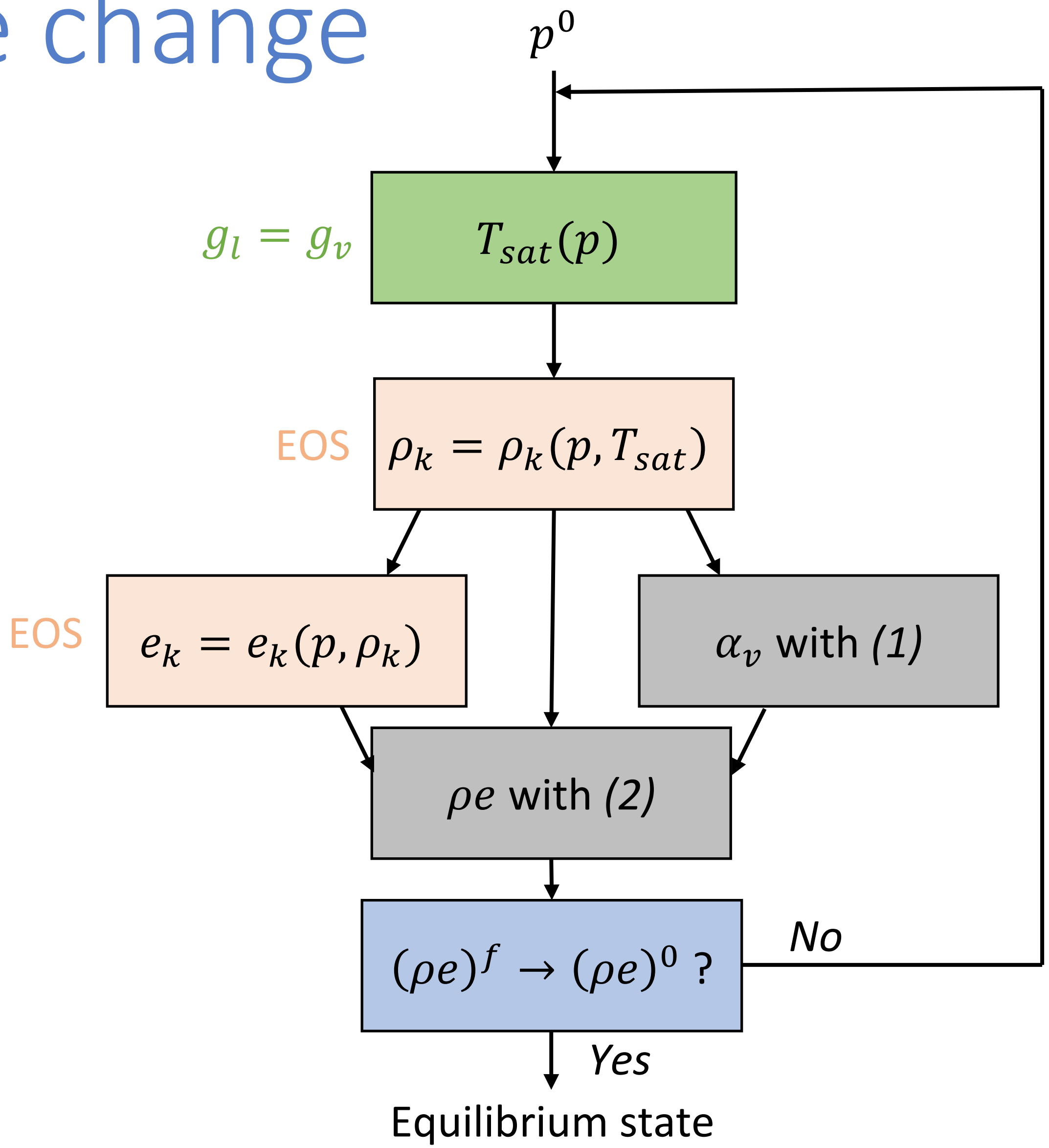

Numerical method: 0D phase change validation

Can we describe the … from a pure phase

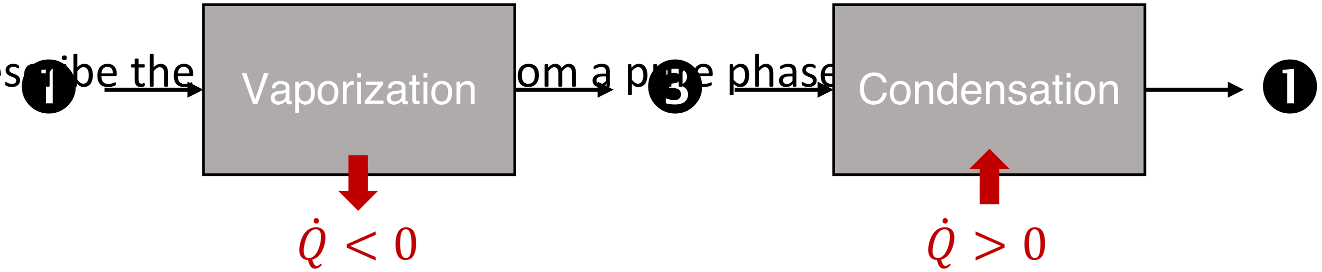

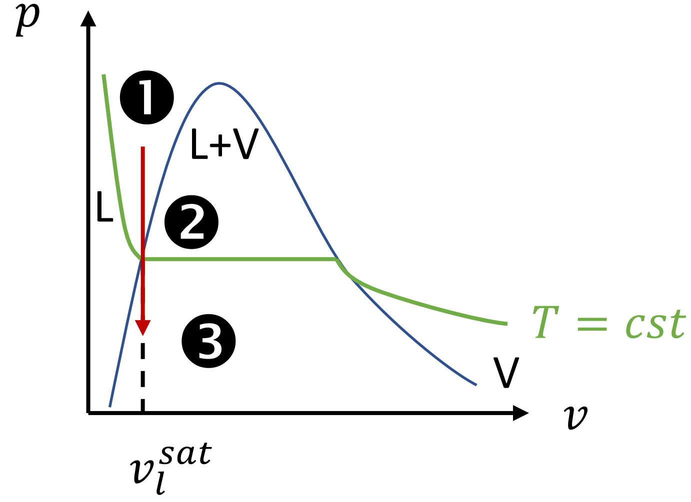

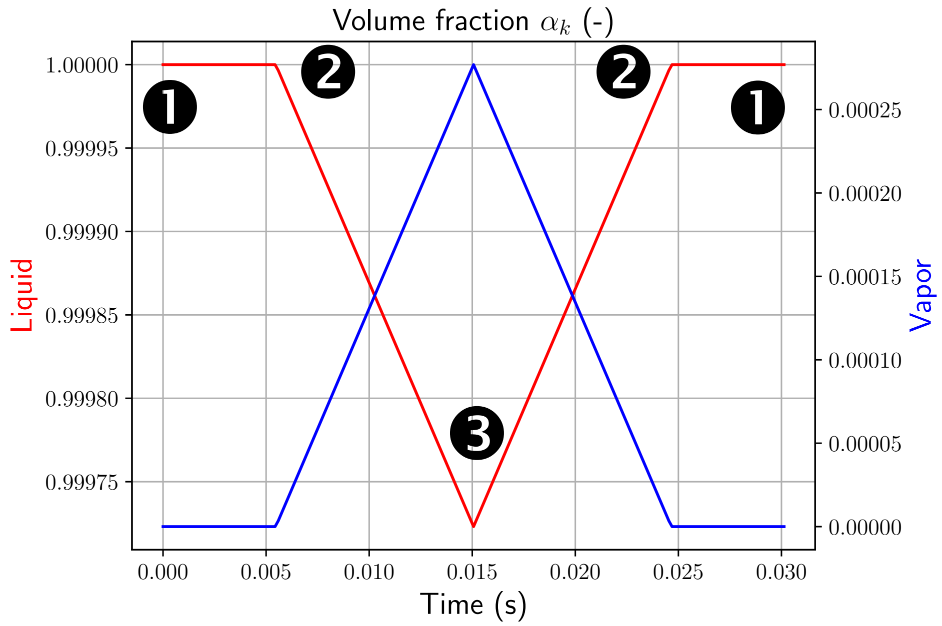

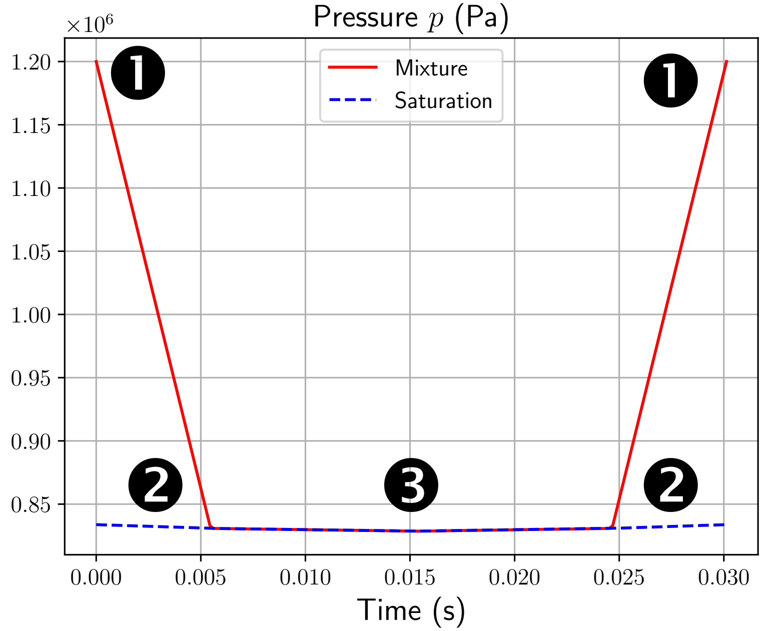

Numerical method: MRF fluxes

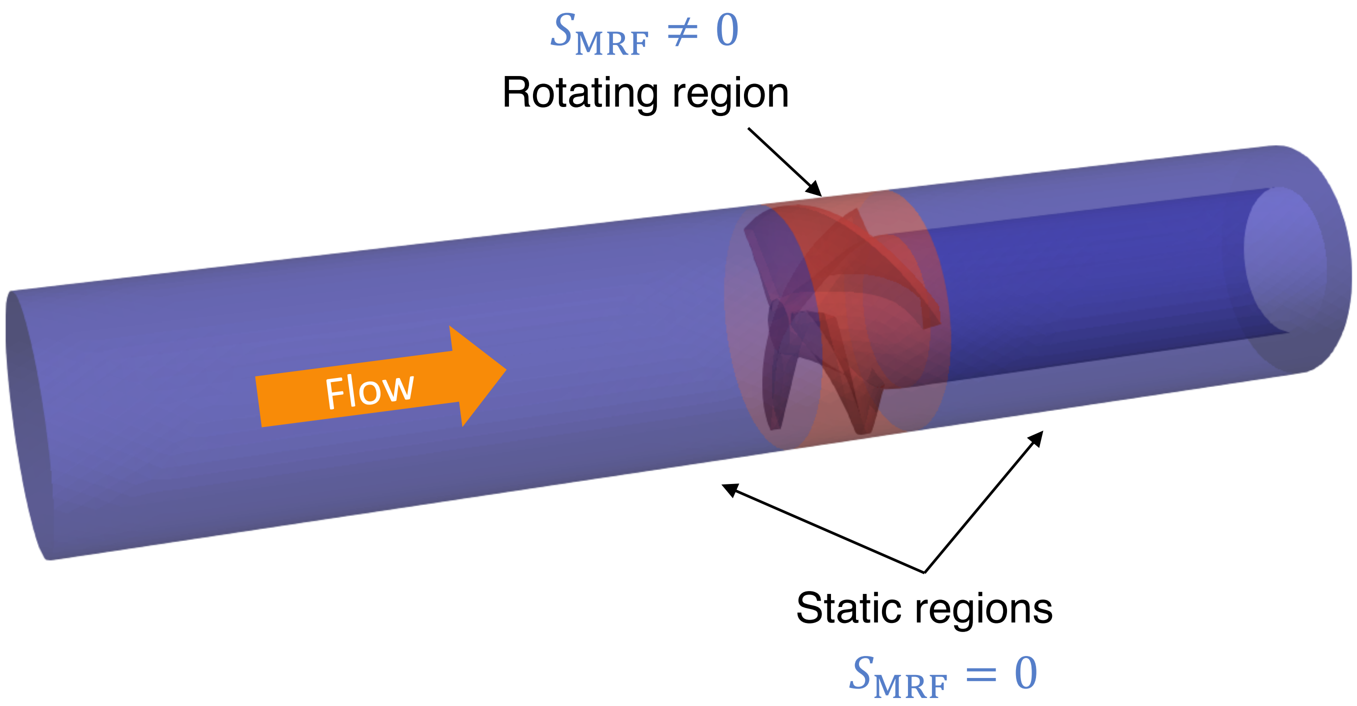

Model in compact form:
$\partial_t U + \nabla \cdot F(U) + \Sigma(U) = R(U) + S_{\mathrm{MRF}}(U)$

Numerical method: MRF fluxes

Modified Riemann problem

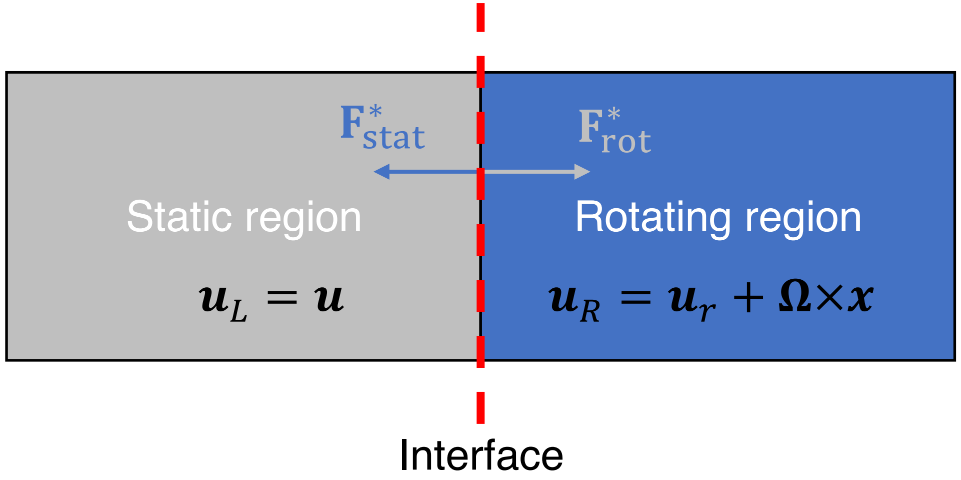

Absolute vel. = Relative vel. + Rot. vel.

$$\boldsymbol{u} = \boldsymbol{u}_r + \boldsymbol{\Omega}\times\boldsymbol{x}$$

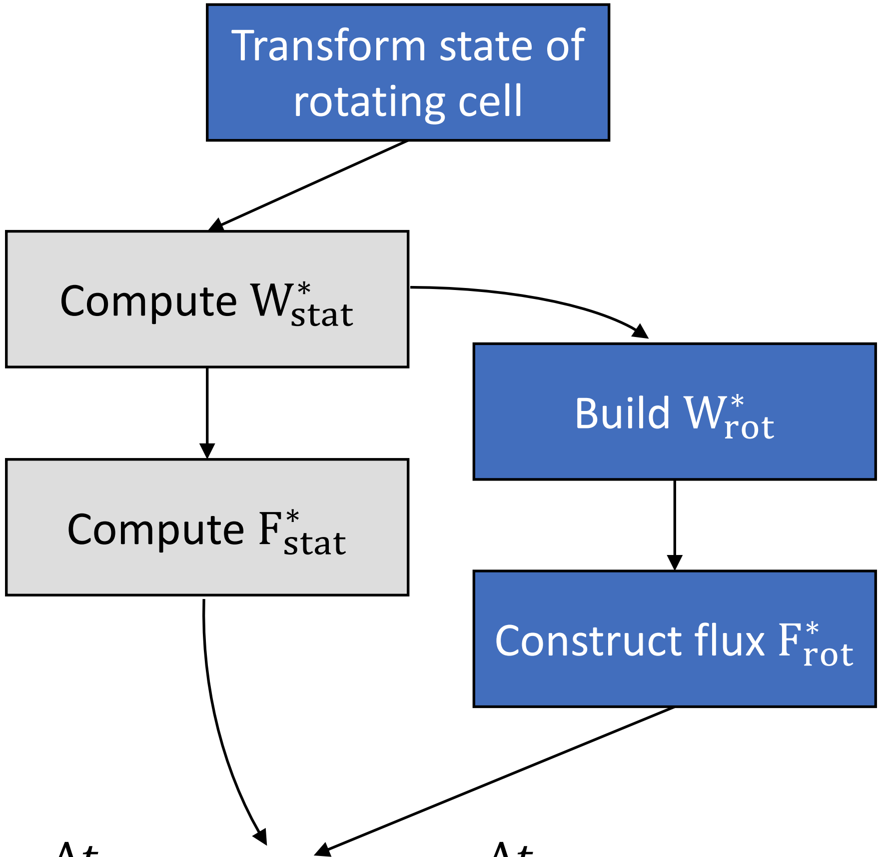

$$\boldsymbol{U}_i^{n+1} = \boldsymbol{U}_i^n - \frac{\Delta t}{V_i}\left(\Sigma_{s=1}^{N_s} A_s \boldsymbol{F}_s^* \cdot \boldsymbol{n}_s\right) - \frac{\Delta t}{V_i} H(\boldsymbol{U}_i^n)\left(\Sigma_{s=1}^{N_s} A_s \boldsymbol{u}_s^* \cdot \boldsymbol{n}_s\right)$$

Numerical method: mesh mapping

Reduce computation time

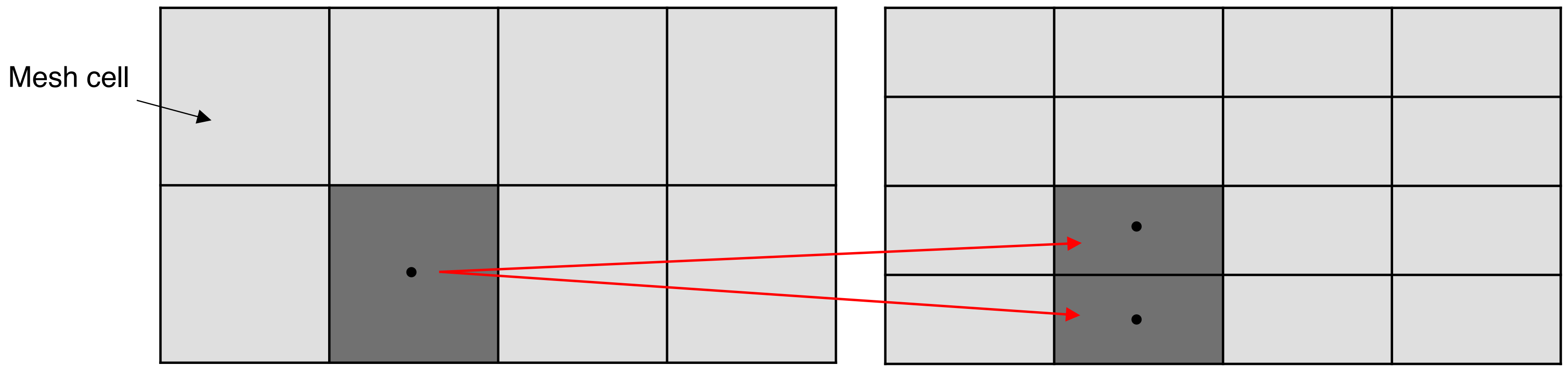

Coarse mesh with steady solution

Fine mesh to initialize

Numerical method: mesh mapping

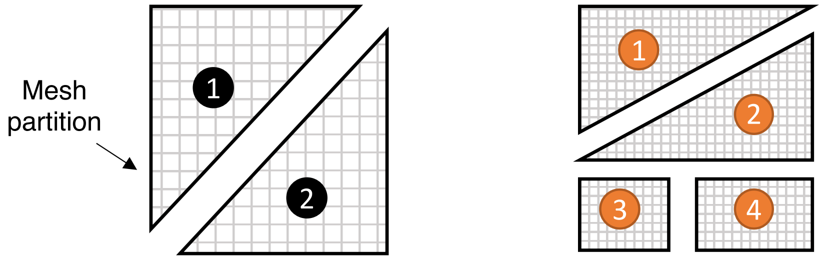

Coarse mesh with
steady solution

Fine mesh to initialize

Search for the closest cell in each partition of
the coarse mesh

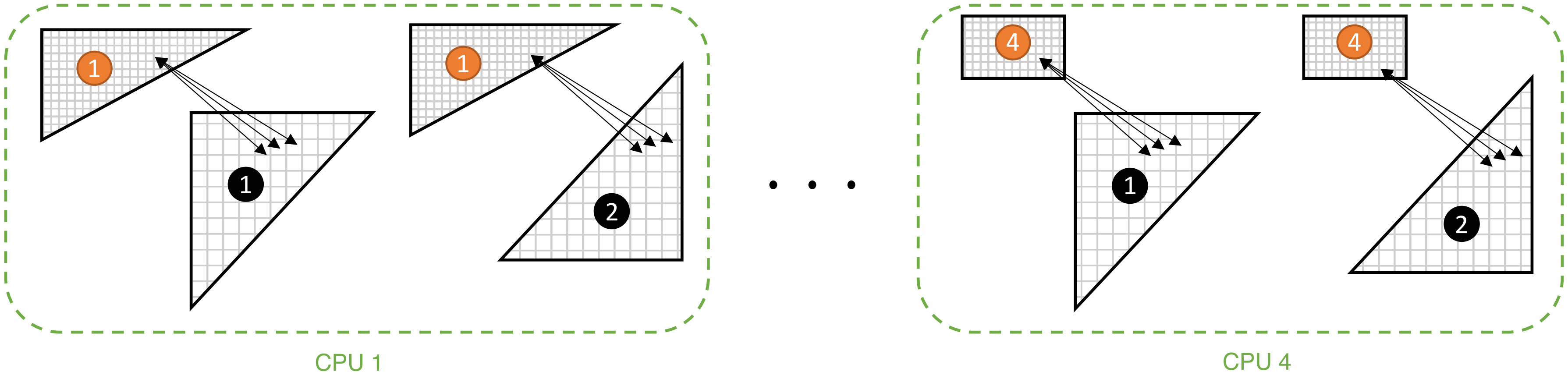

Numerical method: mesh mapping validation

Inflow
$H_0 = H_0(p_0, \rho_0)$
$p_0 = 1$ bar
$\rho_0 = 1000$ kg.m^{-3}
$\dot{m}_s = 7000$ kg.s^{-1}.m^{-2}

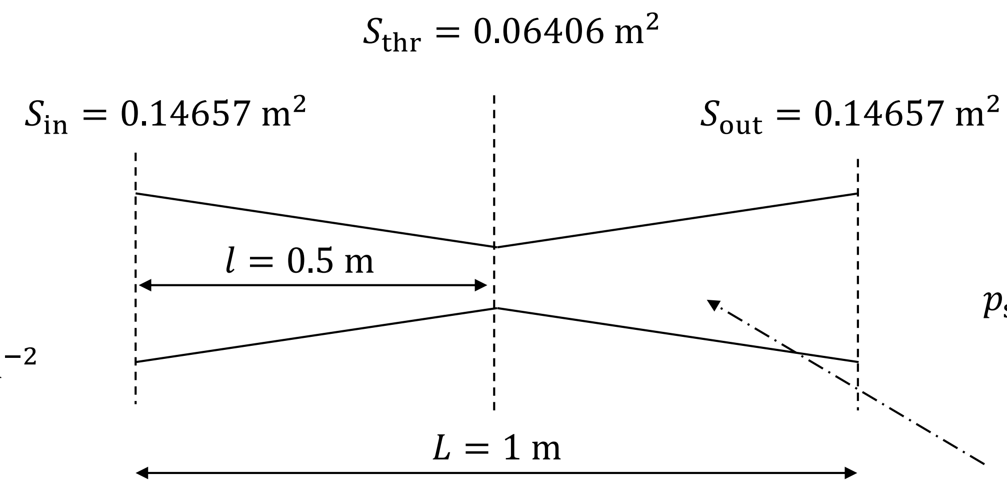

Outlet
$p_s = 1$ bar

Fluid
Liquid water with *SG EOS*
$\gamma = 4.4$
$p_\infty = 600$ MPa

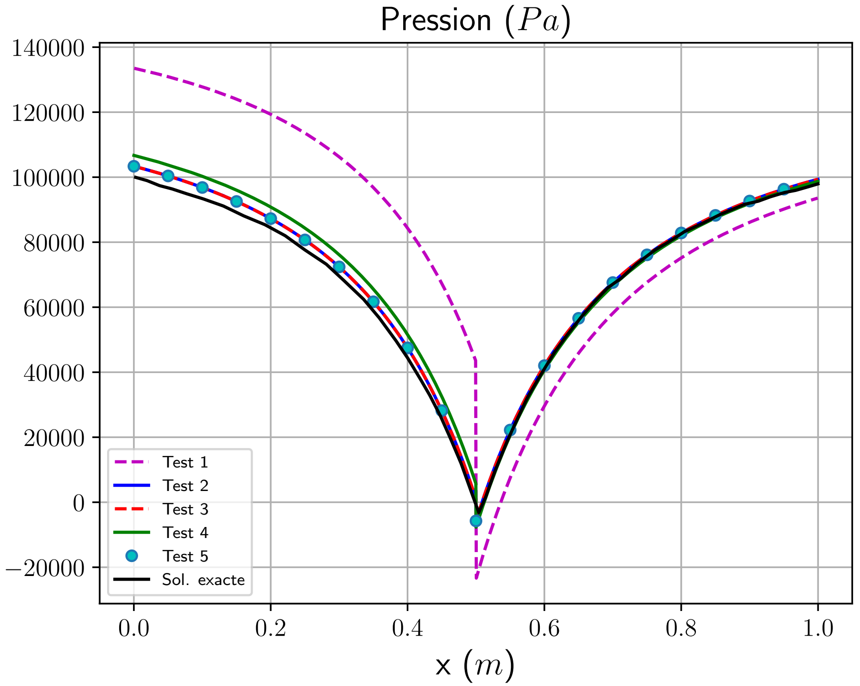

Test	Mesh	Setup	CPUs	$t_{\text{simu}}/t_{\text{réf}}$	$t_{\text{tot}}/t_{\text{réf}}$
1	1000	Normal	1	1	1
2	10 000	Normal	10	15	**15**
3	10 000	Mapping on 1	10	8	**9**

Mapping 41% faster

Summary

Introduction

Modeling of the cavitation phenomenon

- State-of-the-art
- Two-phase flow approach
- Two-phase flow model
- Blades motion

Numerical method

- Numerical scheme
- MRF fluxes
- Mesh mapping

Results

- Test case setup
- Single-phase flow behavior: pump characteristic
- Two-phase flow: cavitating regime

Conclusions & perspectives

Results: test case setup

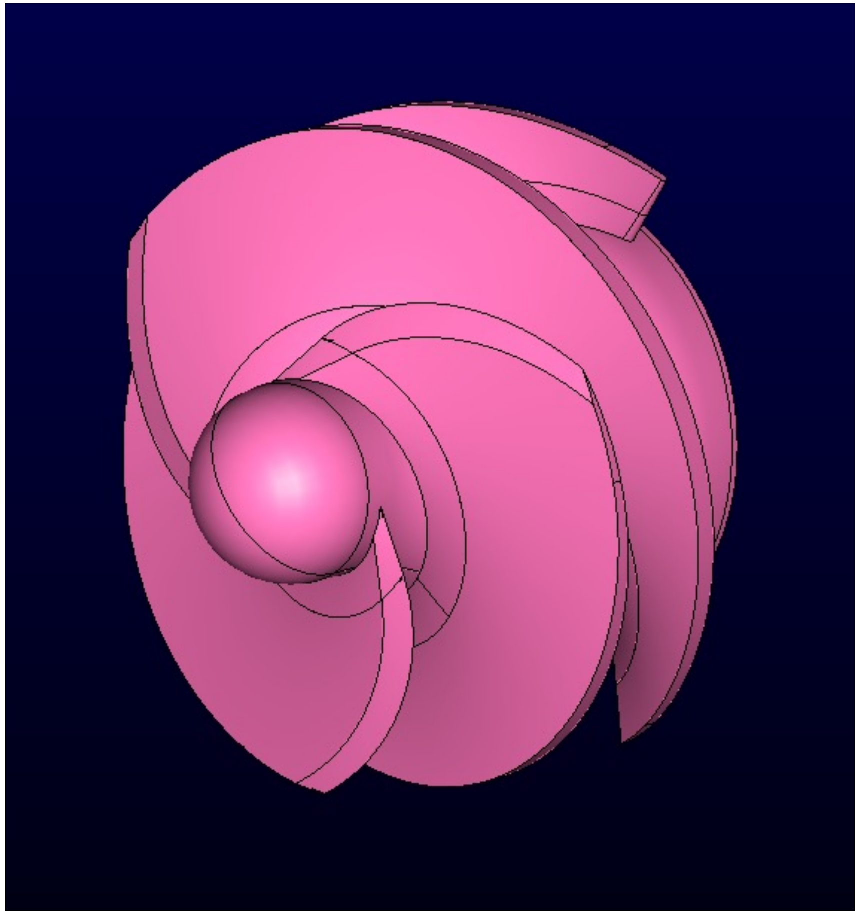

- 3 bladed-inducer
- Variable section hub
- Experimental data from

CREMHyG

Results: test case setup

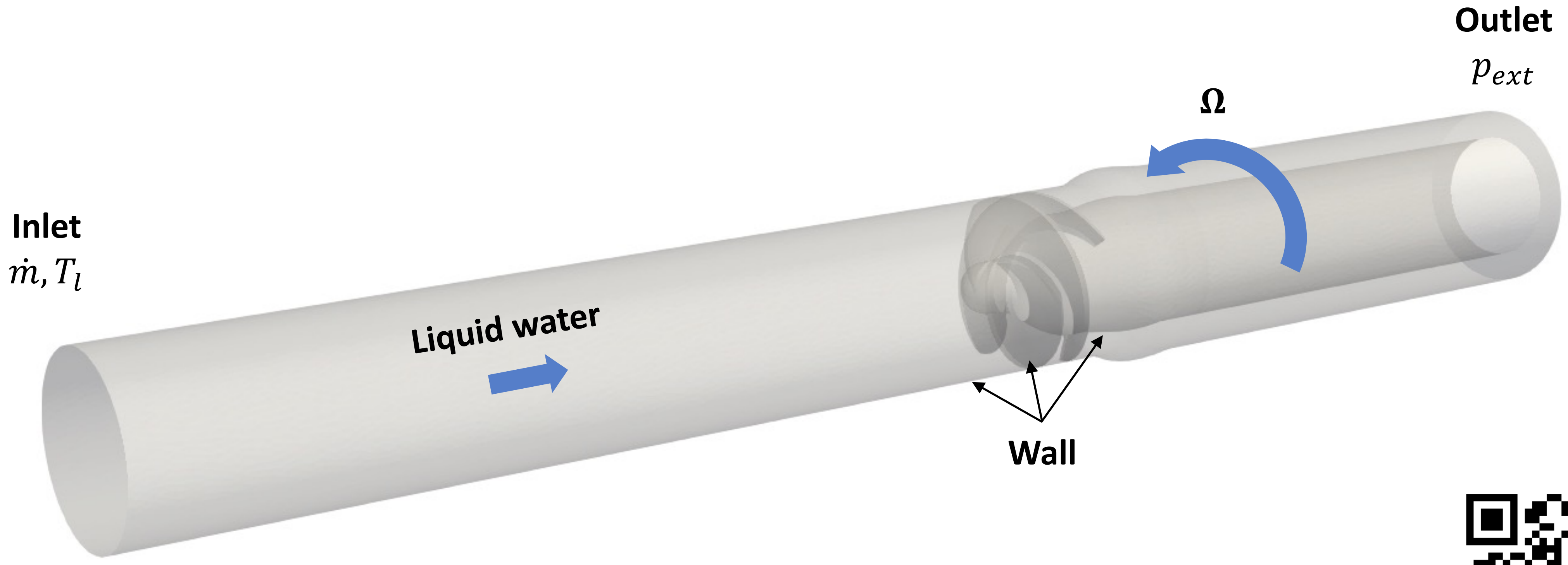

Numerical implementation in the open-source CFD solver **ECOGEN**

Results: mesh convergence

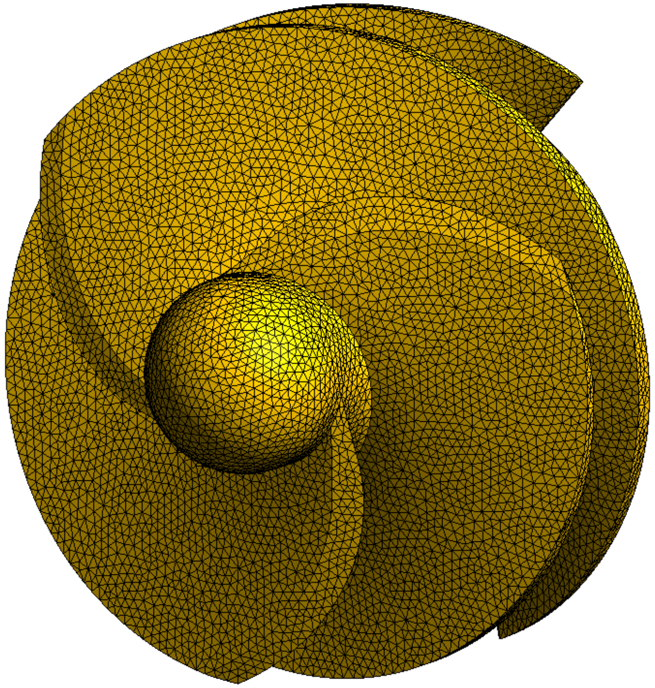

919k cells

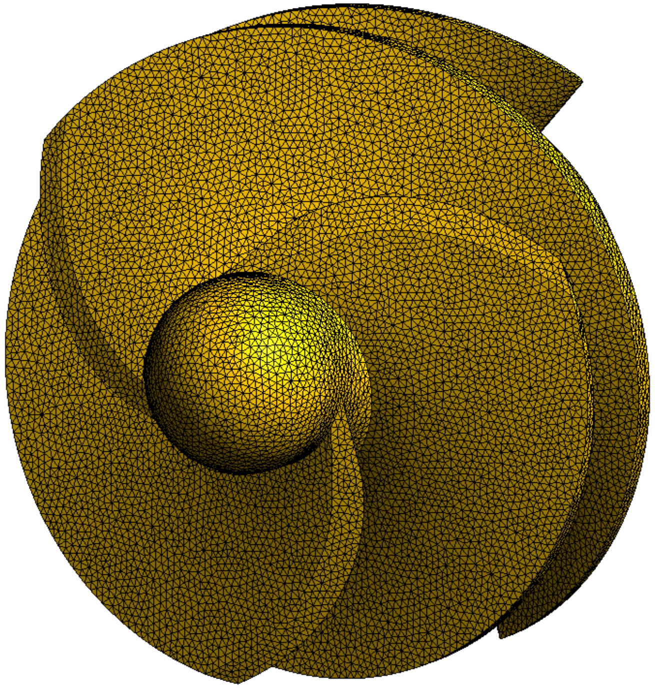

1M527k cells

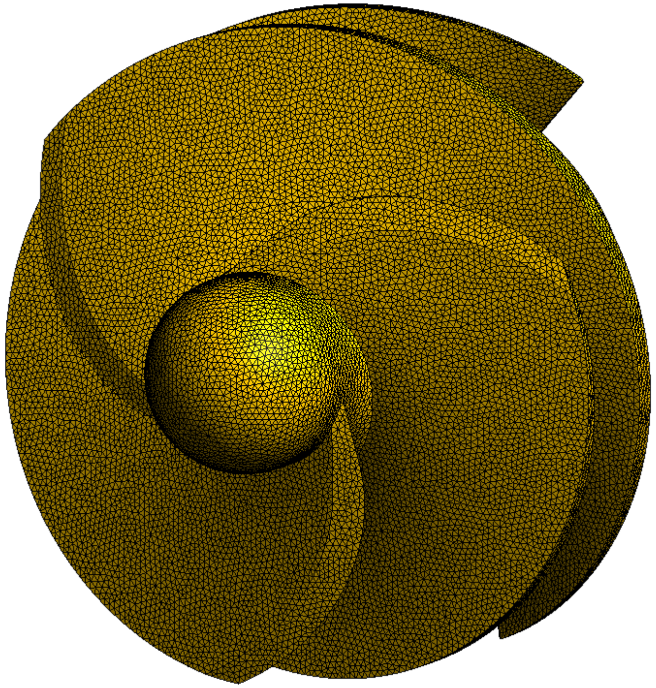

2M543k cells

Results: mesh convergence

- Nominal mass flow rate $\dot{m} = \dot{m}_n$
- Pressure measured at the wall averaged in time/space

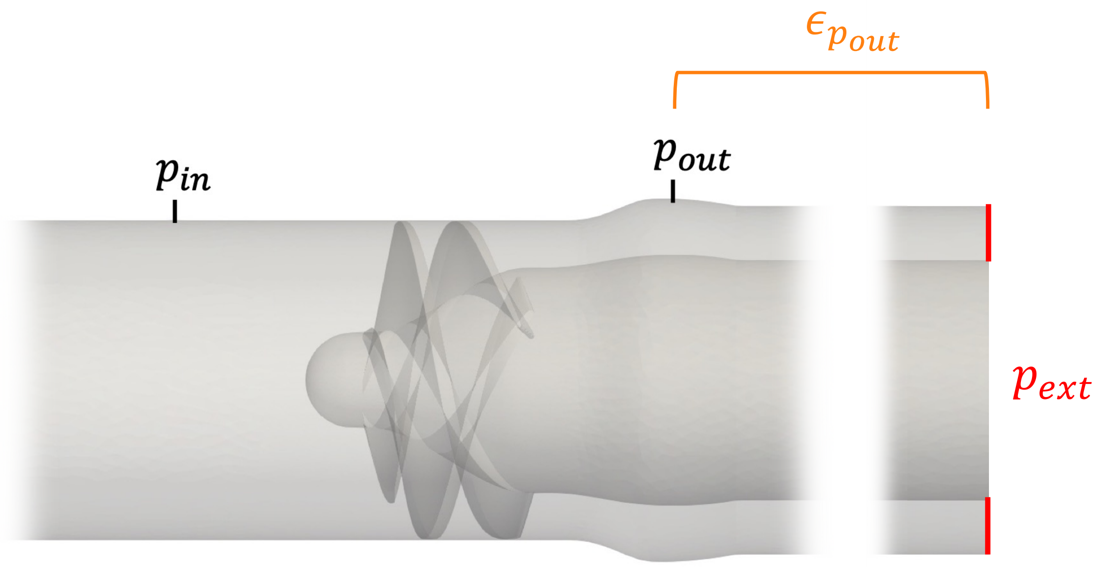

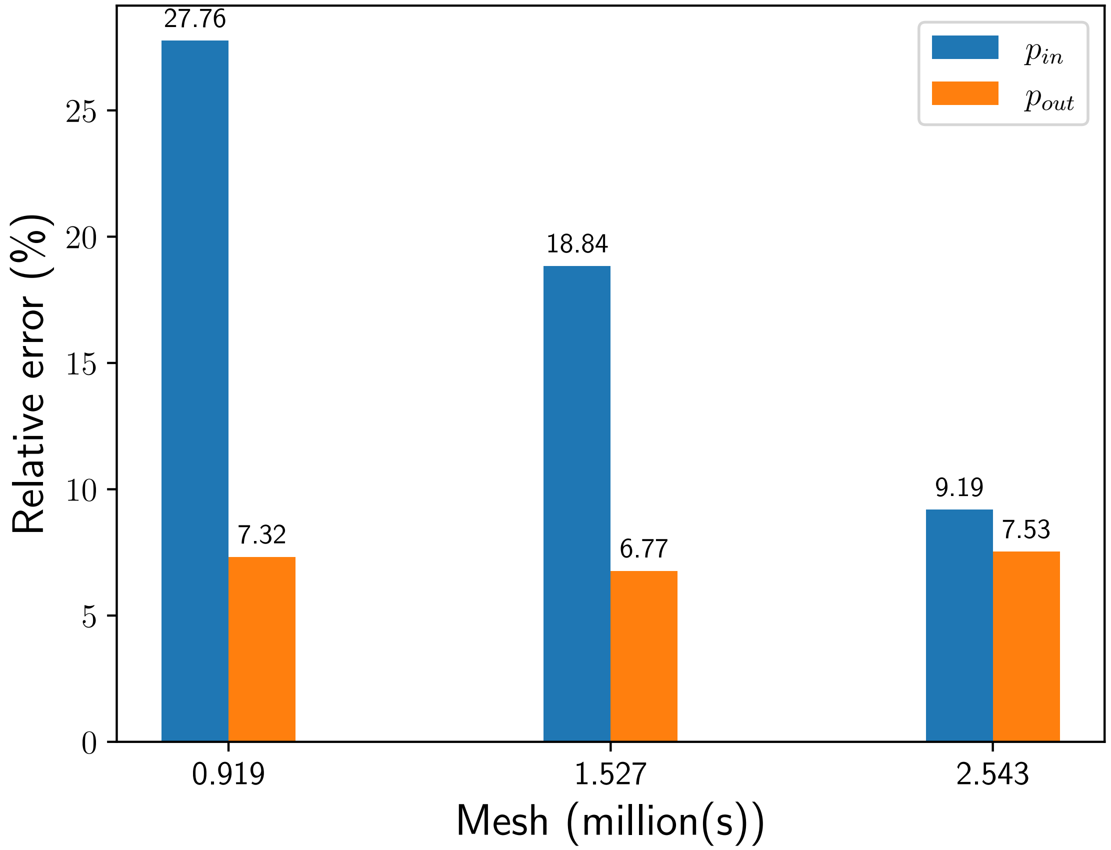

Results: mesh convergence

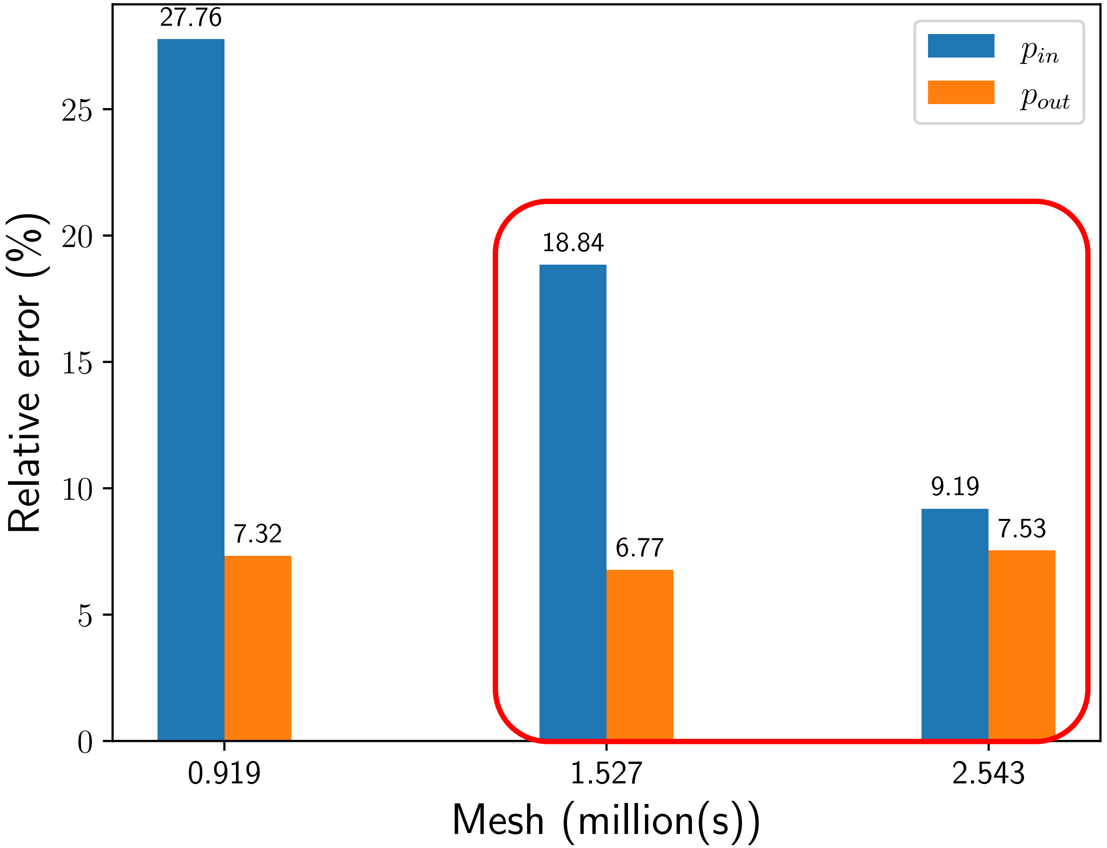

Mesh (millions)	1.527	2.543
Number of CPUs	160	256
Computation time (h)	152	157
CPU time (h)	24440	40192

Trade-off between computationnal ressources / error

Summary

Introduction

Modeling of the cavitation phenomenon

- State-of-the-art
- Two-phase flow approach
- Two-phase flow model
- Blades motion

Numerical method

- Numerical scheme
- MRF fluxes
- Mesh mapping

Results

- Test case setup
- Single-phase flow behavior: pump characteristic
- Two-phase flow: cavitating regime

Conclusions & perspectives

Results: single-phase flow behavior

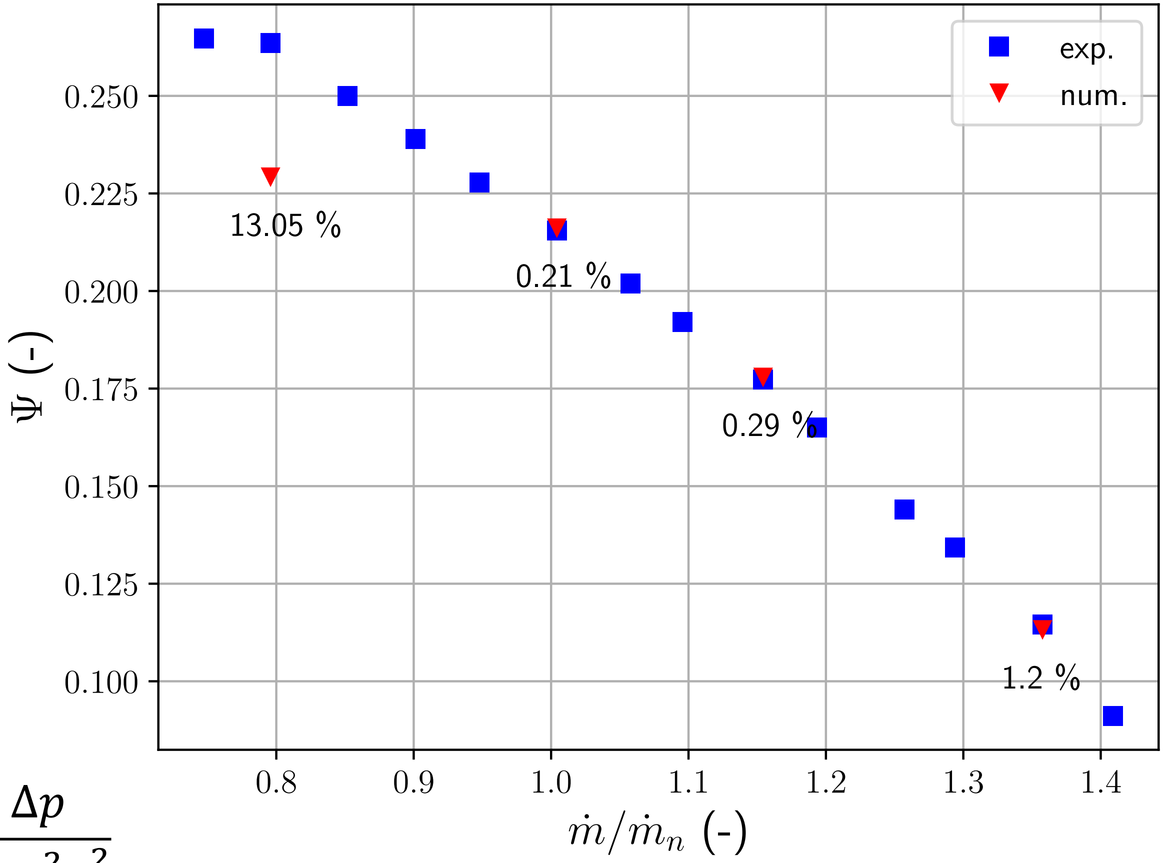

$$\Psi = \frac{\Delta p}{\rho_l \omega^2 r_b^2}$$

Flow rate variation $\dot{m}/\dot{m}_n$

➡ Good match except at low mass flow rate

Results: single-phase flow behavior

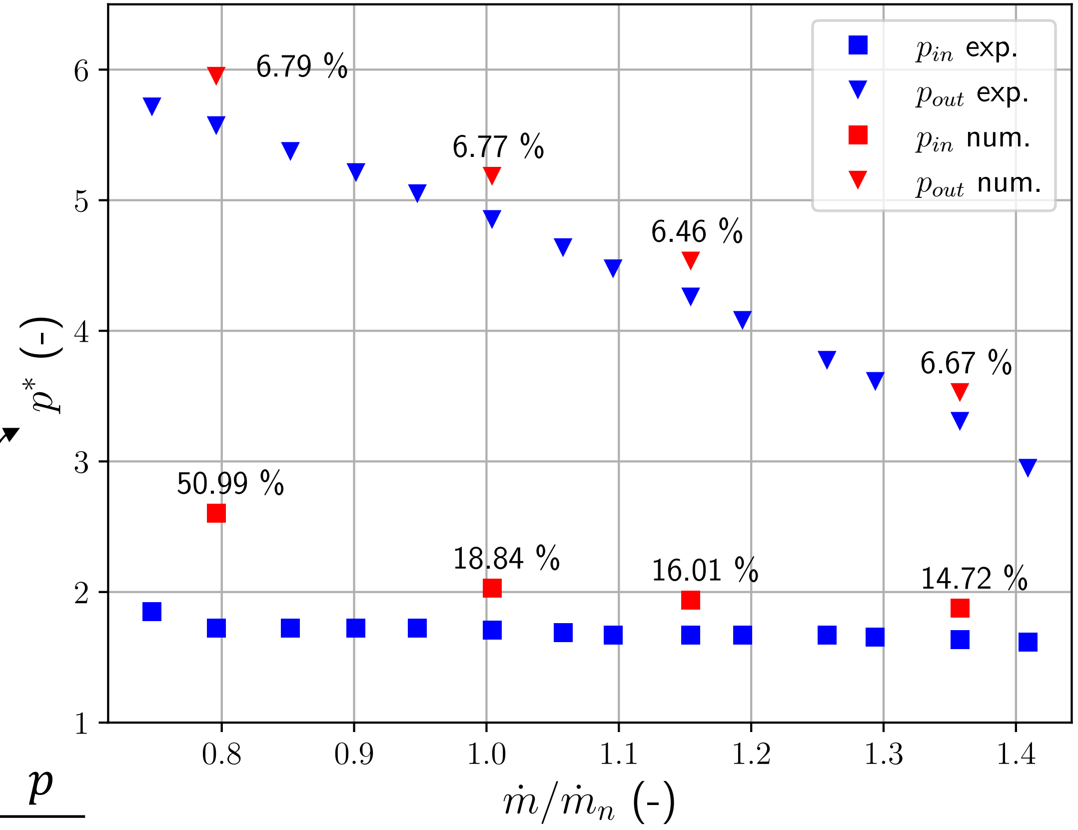

$$p^* = \frac{p}{p_{ref}}$$

Flow rate variation $\dot{m}/\dot{m}_n$

Pressures are overestimated but the inlet/outlet gap is relatively constant except at low massflow rate

Results: single-phase flow behavior

Overpressure error

Low pressure region

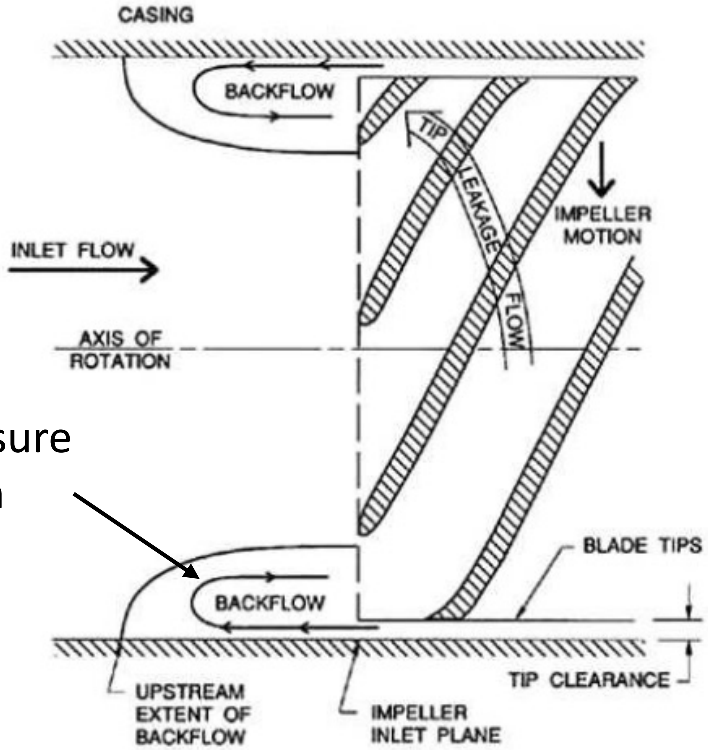

Fig – Illustration of backflow cavitation [Brennen, 2011]

Fig – Backflow cavitation on SSME LOx inducer [Braisted, 1980]

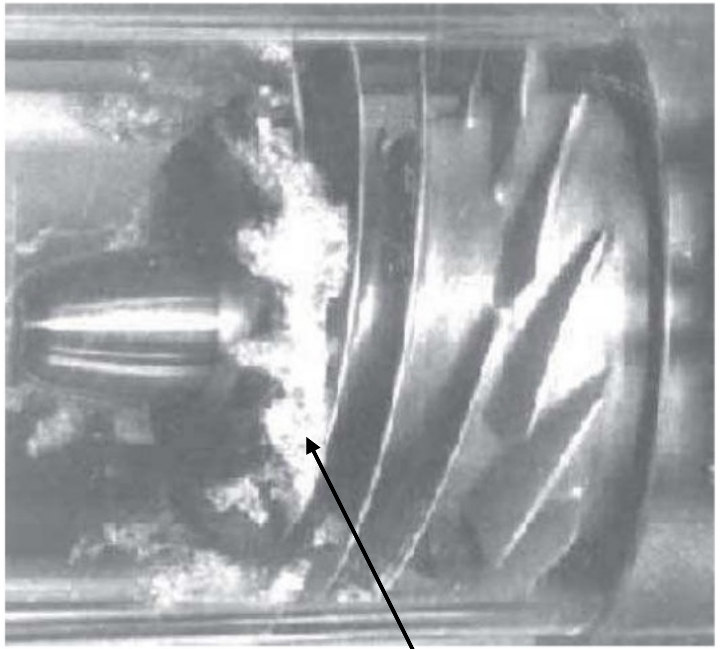

Cavitation at blade tip

Results: single-phase flow behavior

Overpressure error

$$u^* = \frac{u_z}{u_n}$$

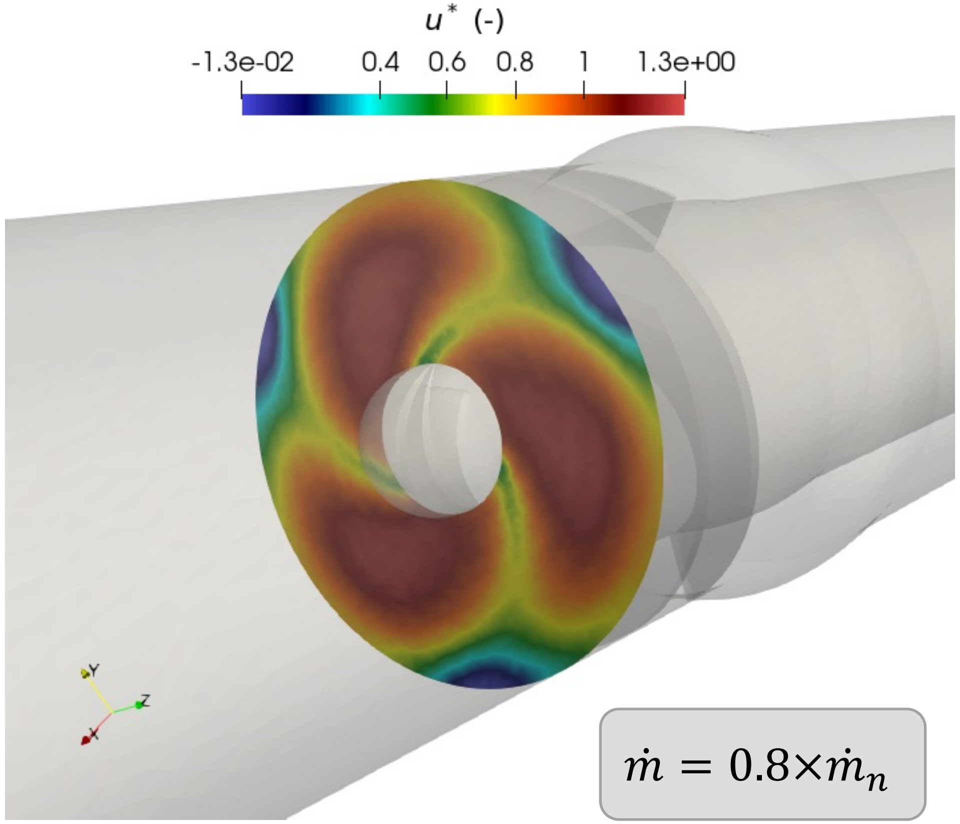

$\dot{m} = 0.8 \times \dot{m}_n$

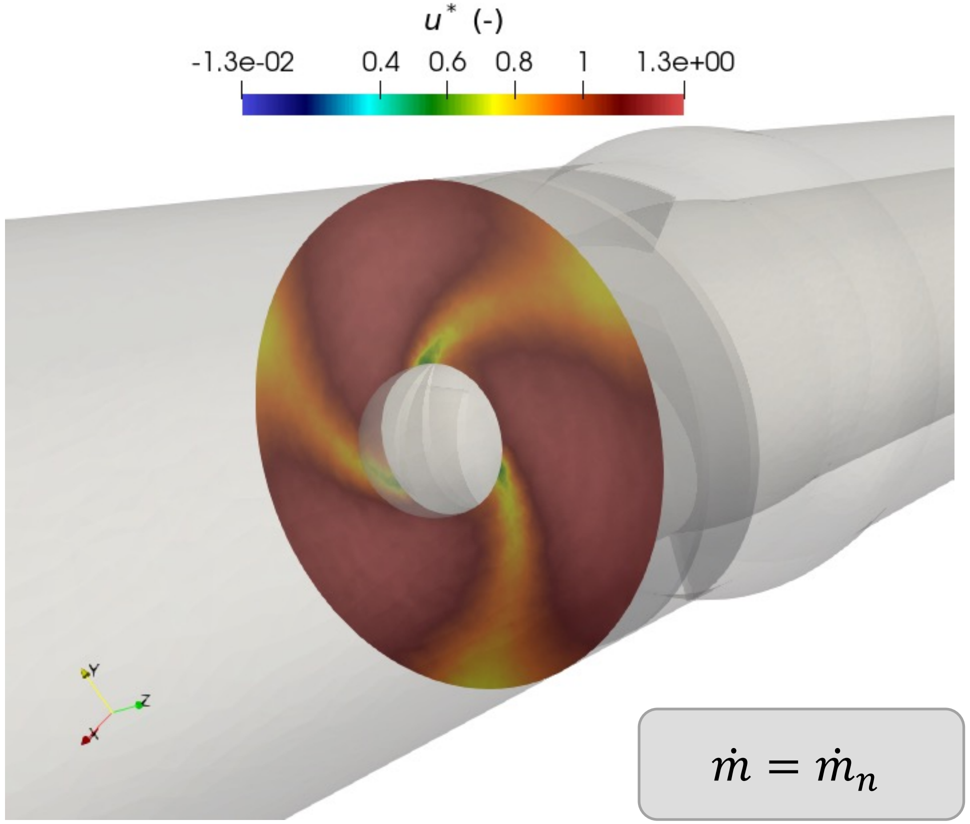

$\dot{m} = \dot{m}_n$

Results: single-phase flow behavior

Study of pressure field

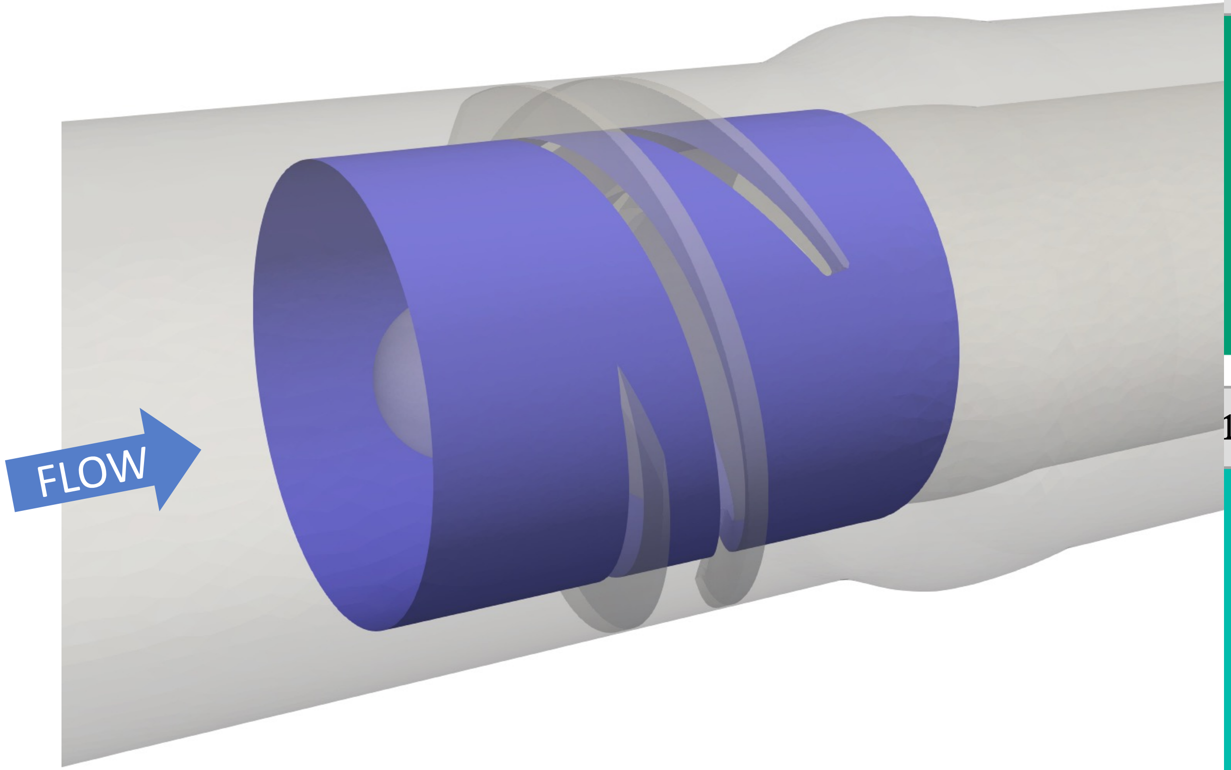

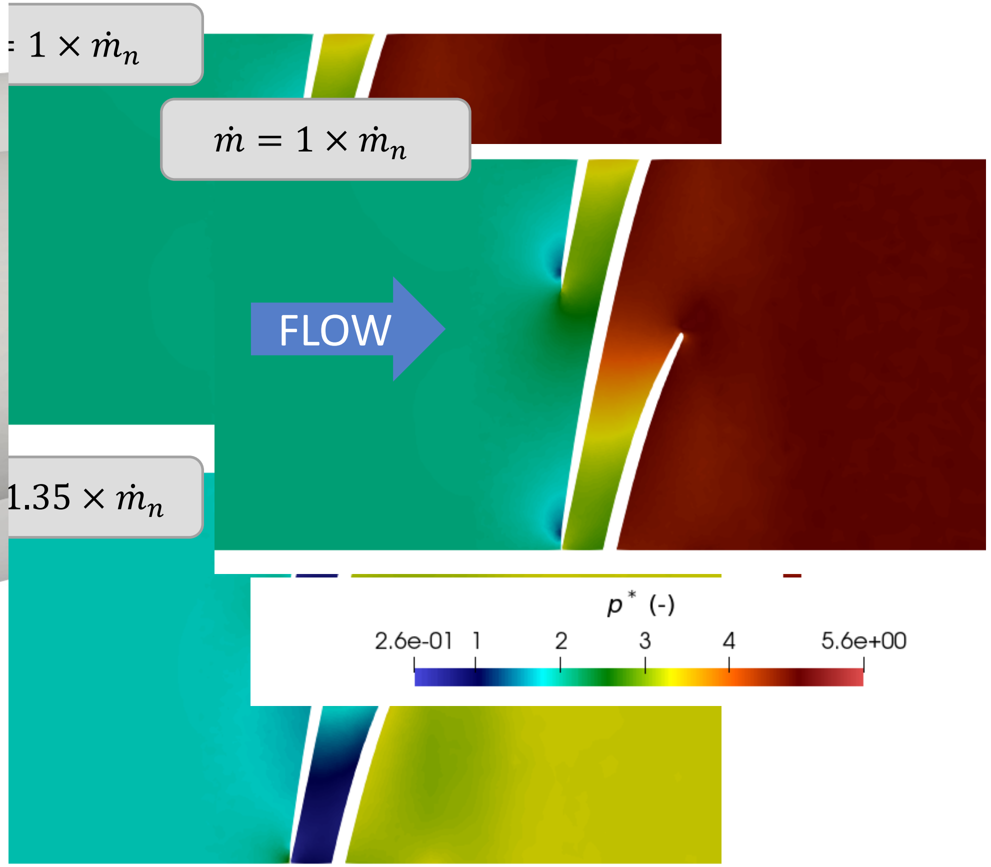

Results: single-phase flow behavior

Blades load

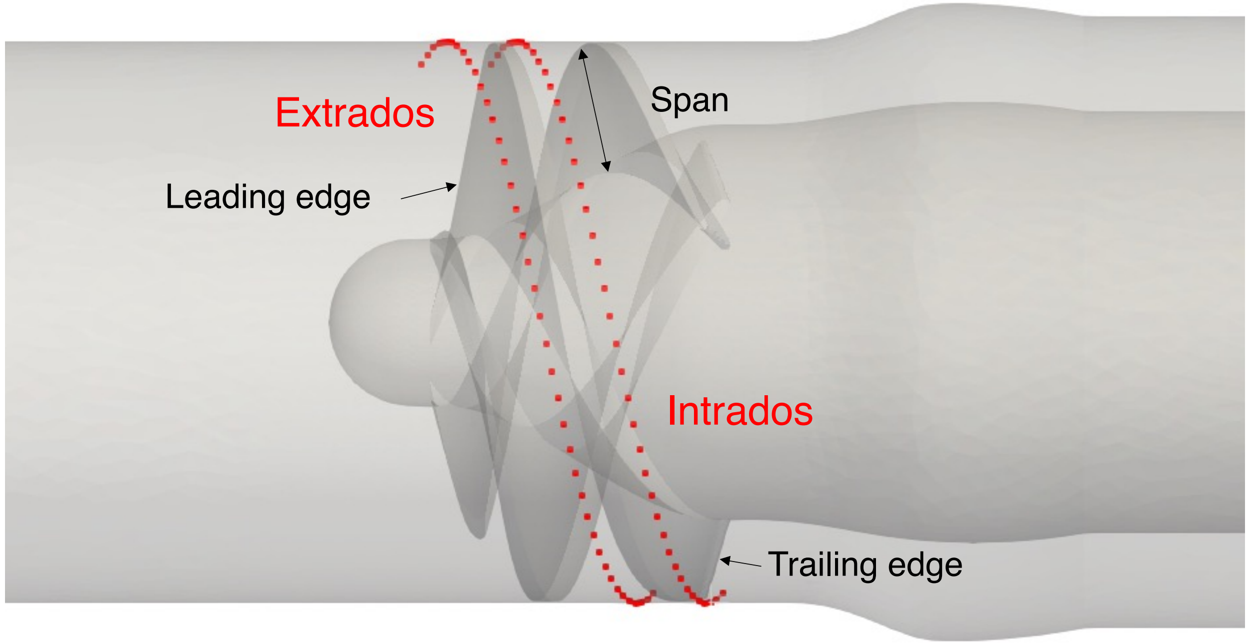

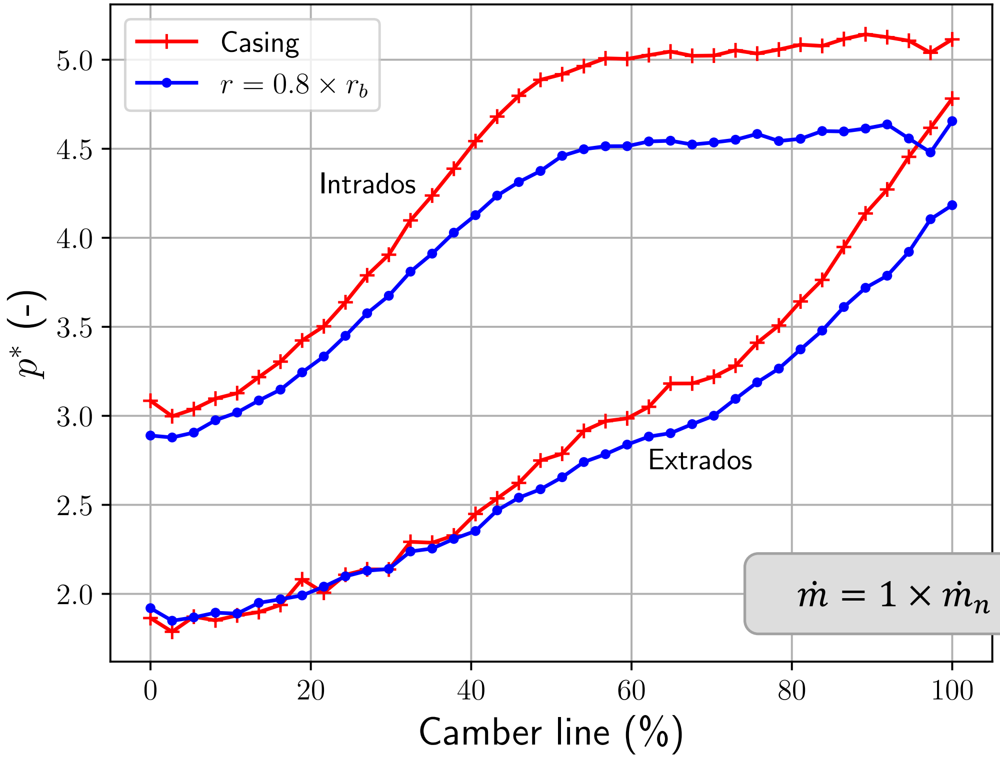

$\dot{m} = 1 \times \dot{m}_n$

Results: single-phase flow behavior

Blades load

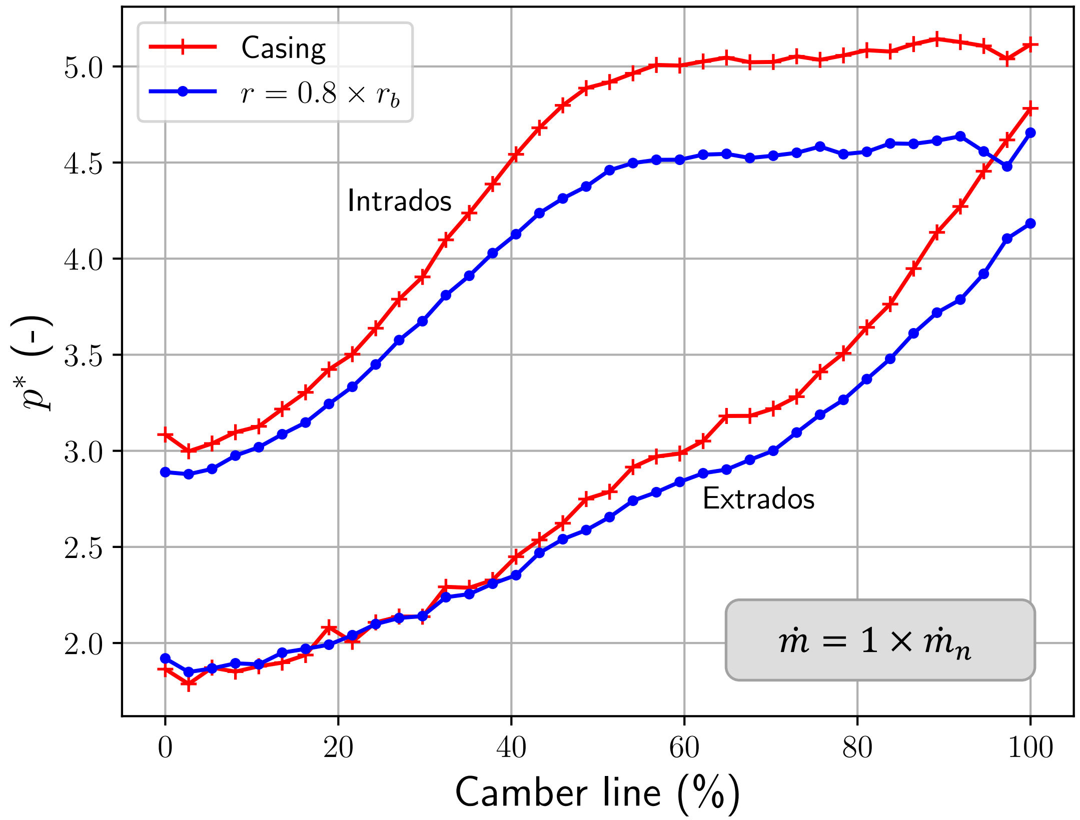

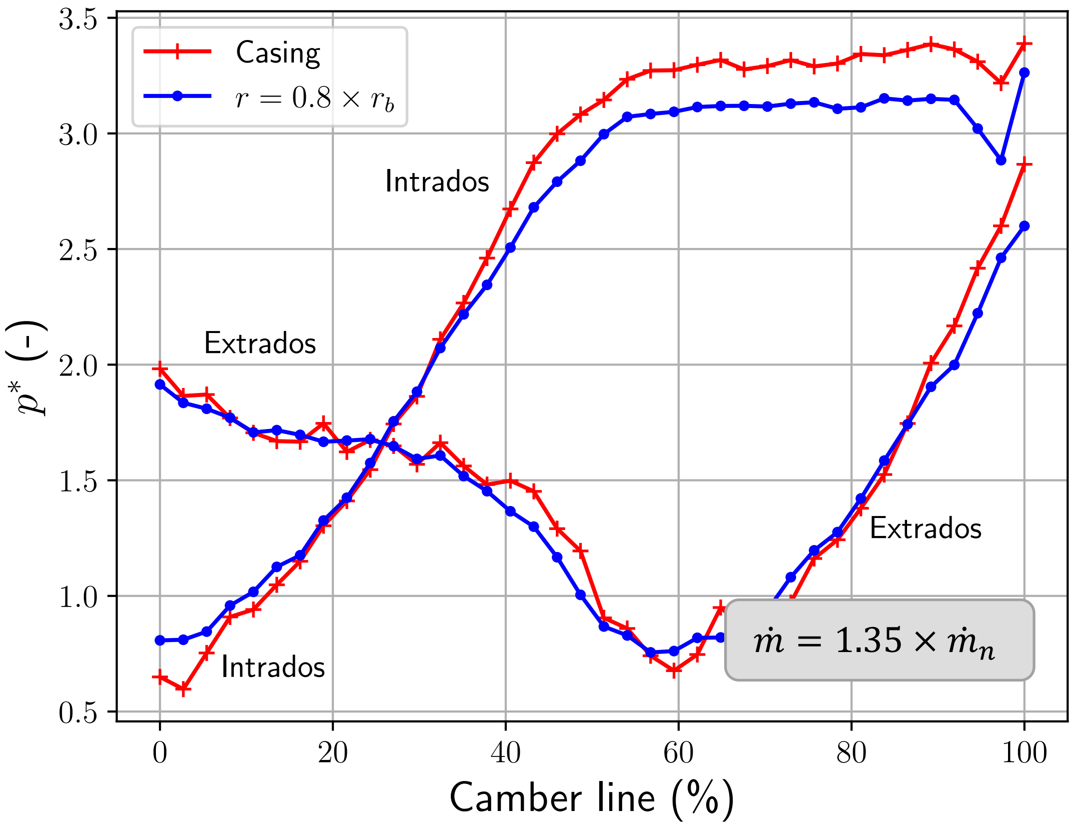

Summary

Introduction

Modeling of the cavitation phenomenon

- State-of-the-art
- Two-phase flow approach
- Two-phase flow model
- Blades motion

Numerical method

- Numerical scheme
- MRF fluxes
- Mesh mapping

Results

- Test case setup
- Single-phase flow behavior: pump characteristic
- Two-phase flow: cavitating regime

Conclusions & perspectives

Results: two-phase flow in cavitating regime

Performance curve

- Variation of the outlet pressure at $\dot{m}_n$
- $\Psi = \frac{\Delta p}{\rho_l \omega^2 r_b^2}$
- $\tau = \frac{p_e^{tot} - p_v}{\rho_l \omega^2 r_b^2}$

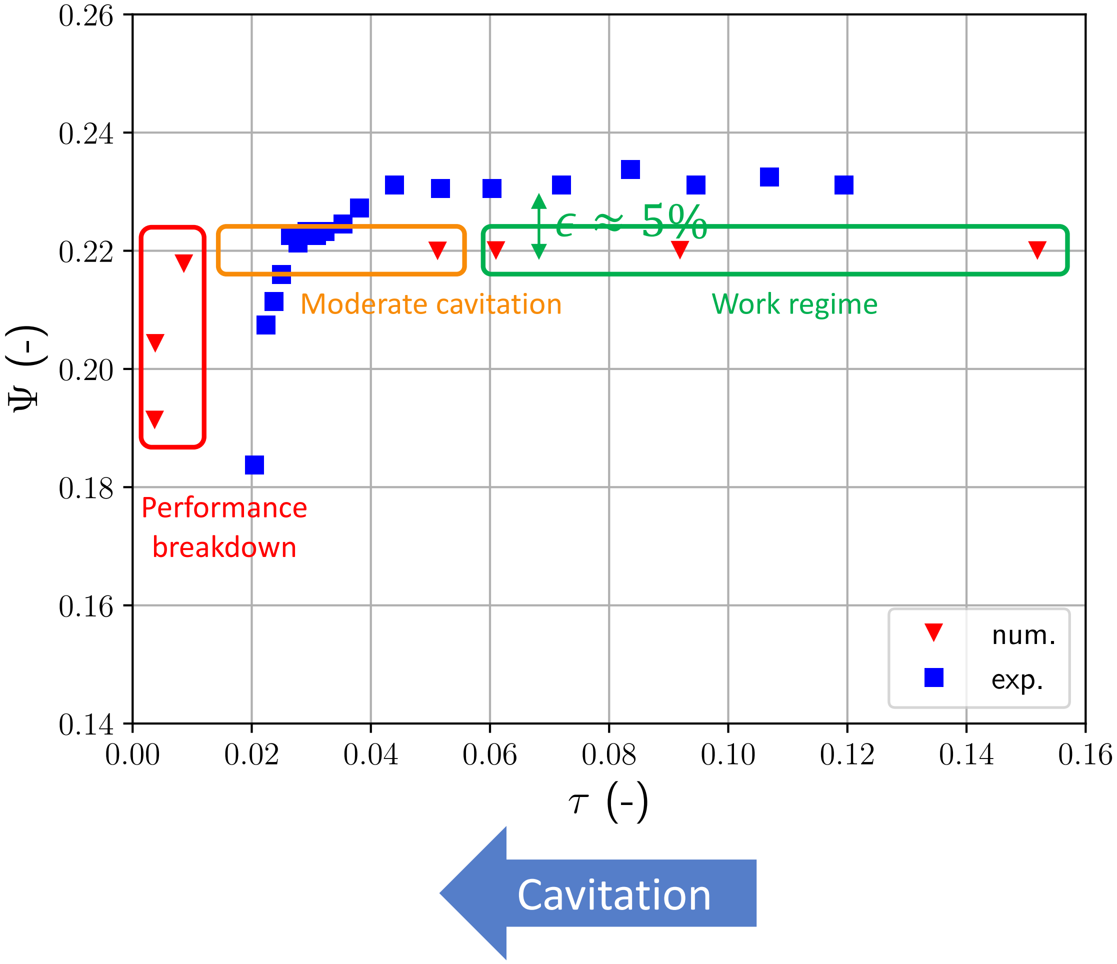

Results: two-phase flow in cavitating regime

Cavitation pockets

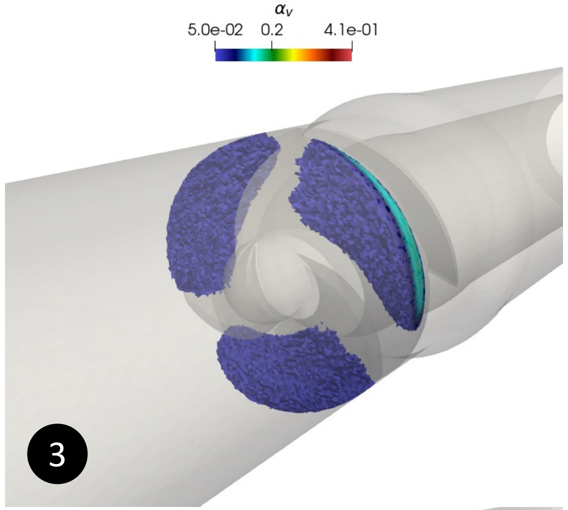

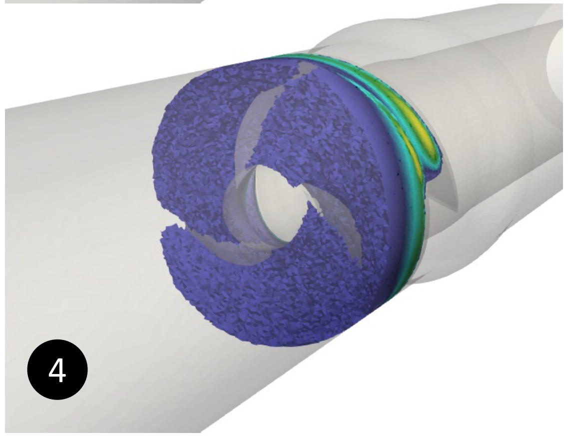

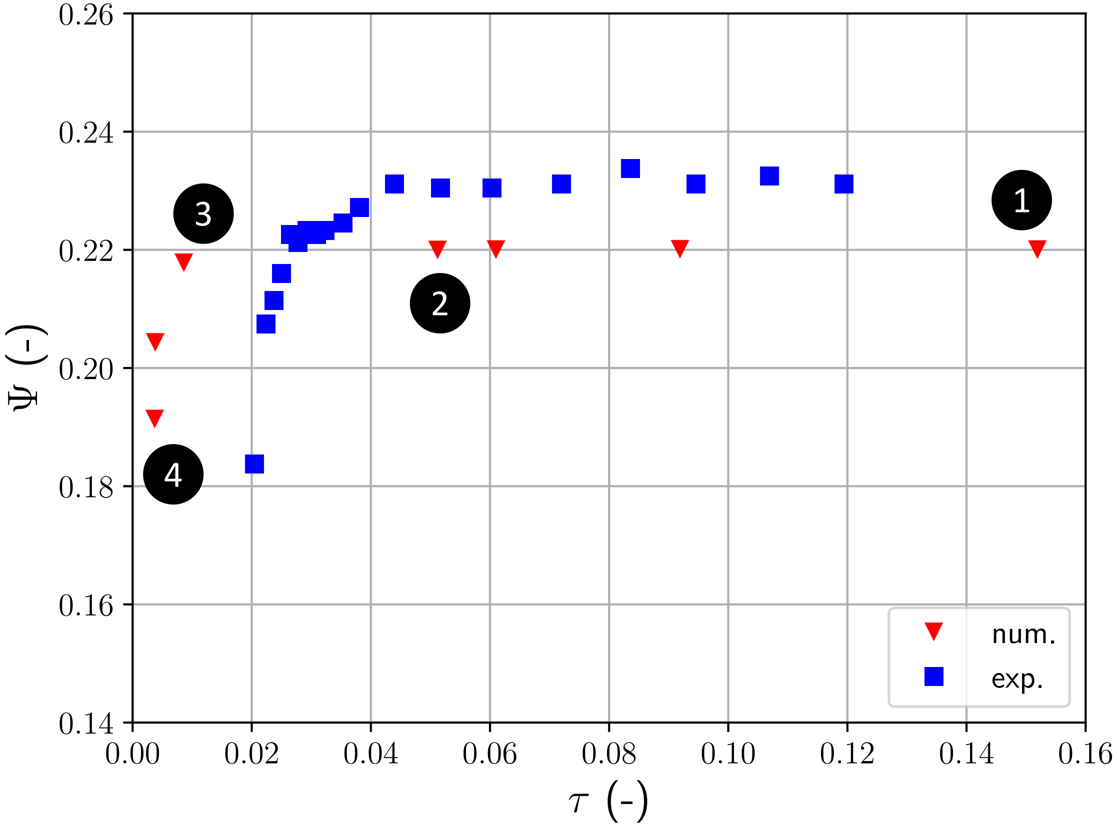

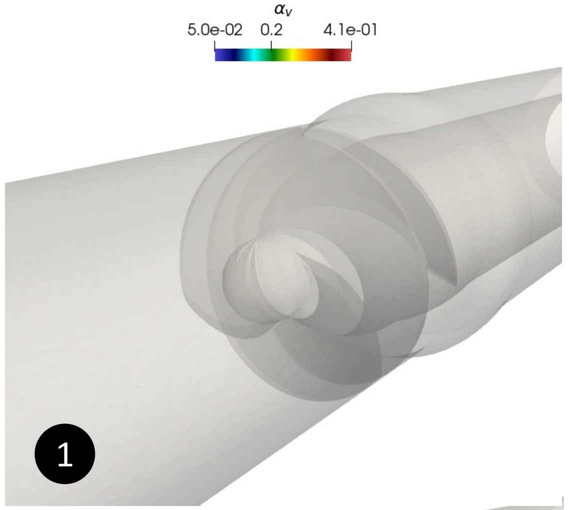

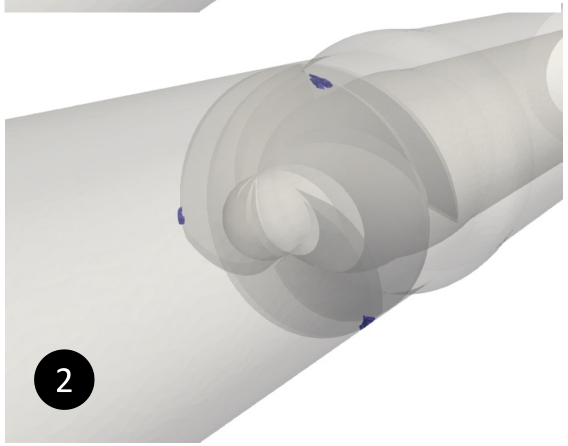

Results: two-phase flow in cavitating regime

Cavitation number estimates

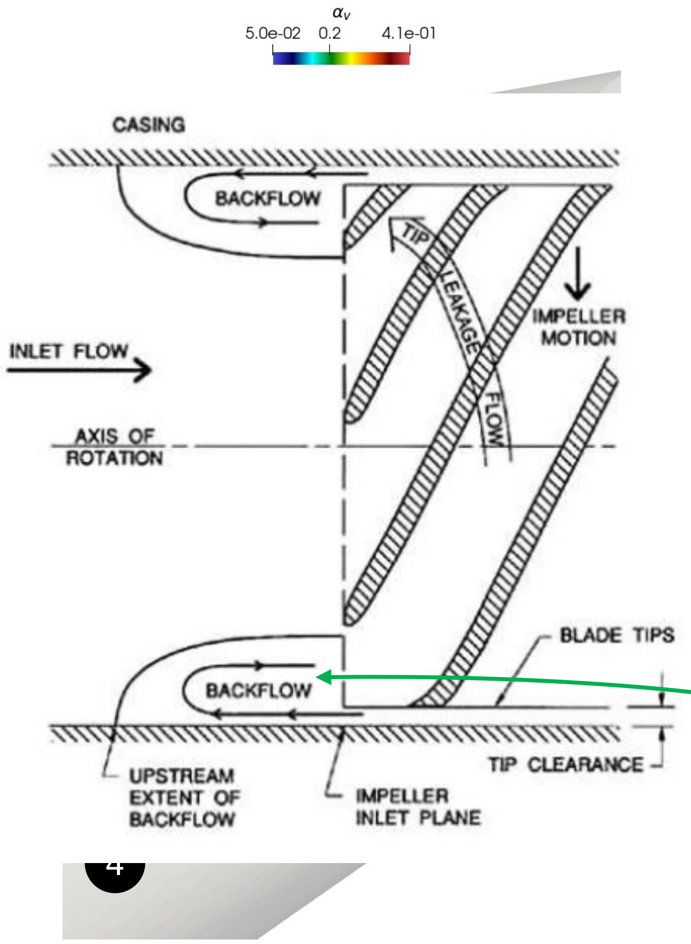

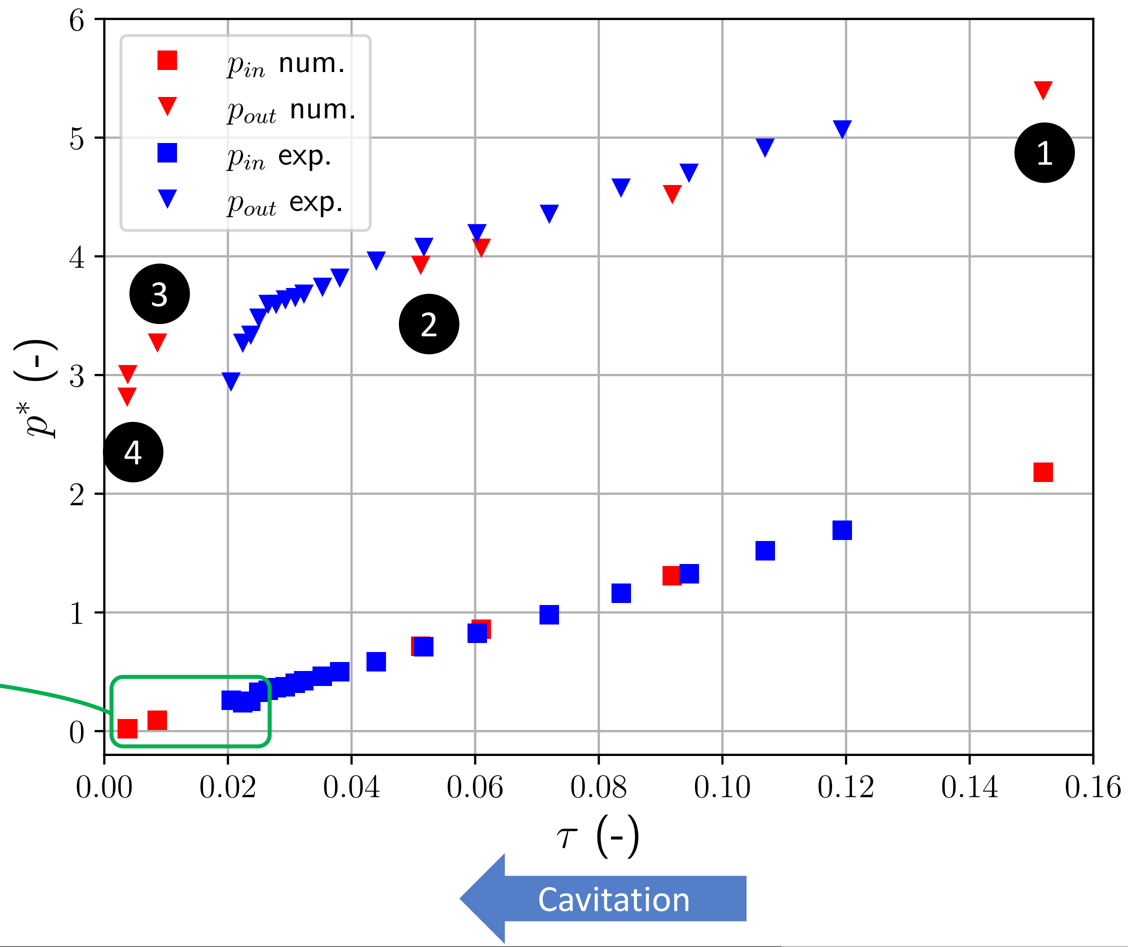

$$\tau = \frac{\boxed{p_e^{tot}} - p_v}{\rho_l \omega^2 r_b^2}$$

$$p^* = \frac{p}{p_{ref}}$$

Results: two-phase flow in cavitating regime

Increase massflow rate $\dot{m} = 1.15 \times \dot{m}_n$

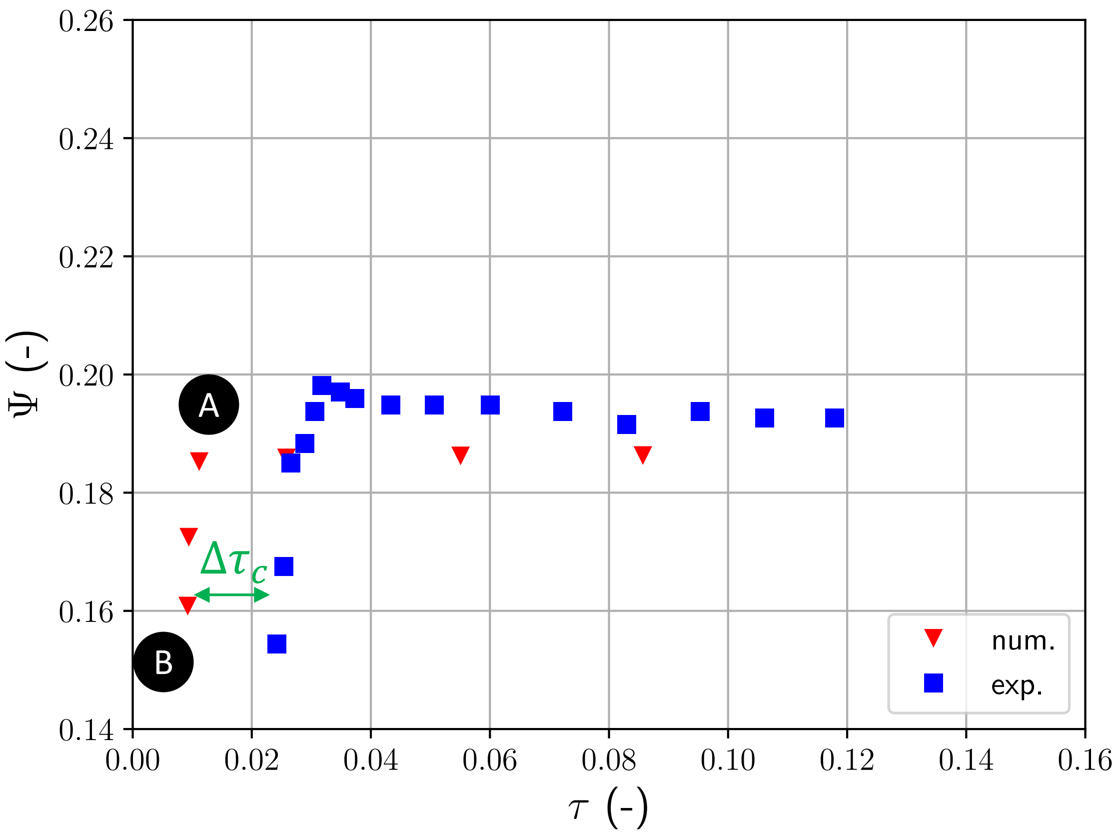

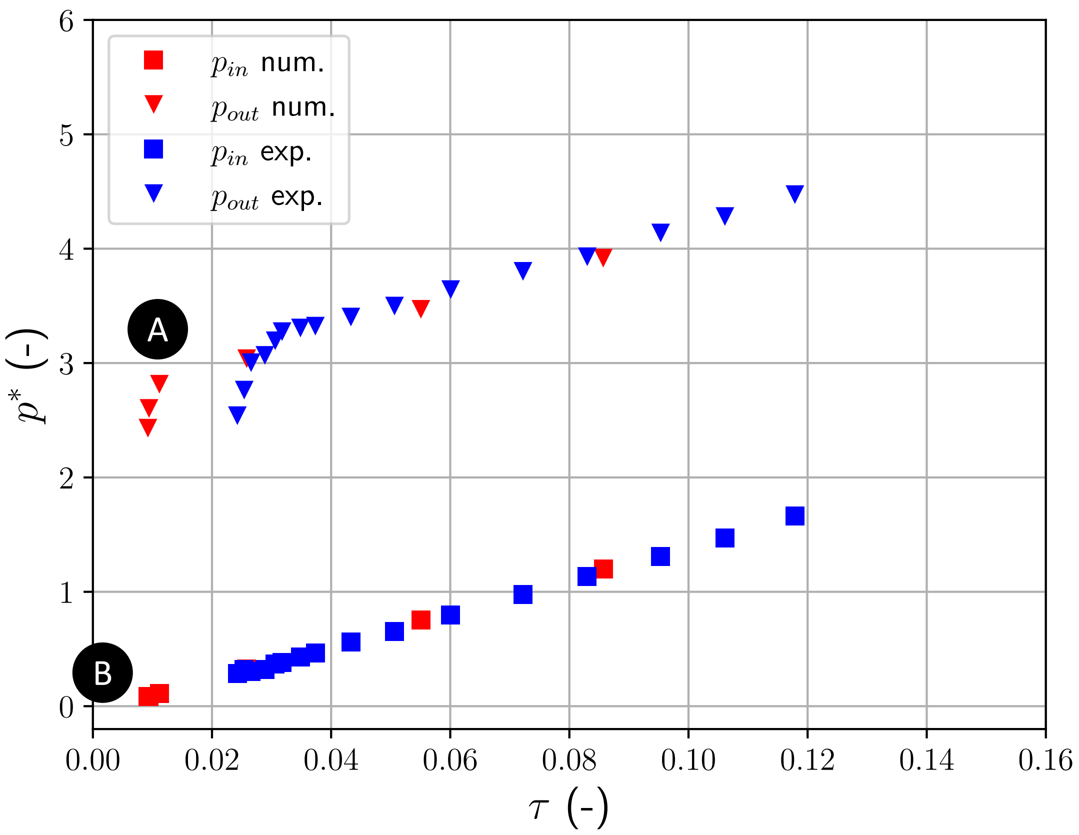

Results: two-phase flow in cavitating regime

Increase massflow rate $\dot{m} = 1.15 \times \dot{m}_n$

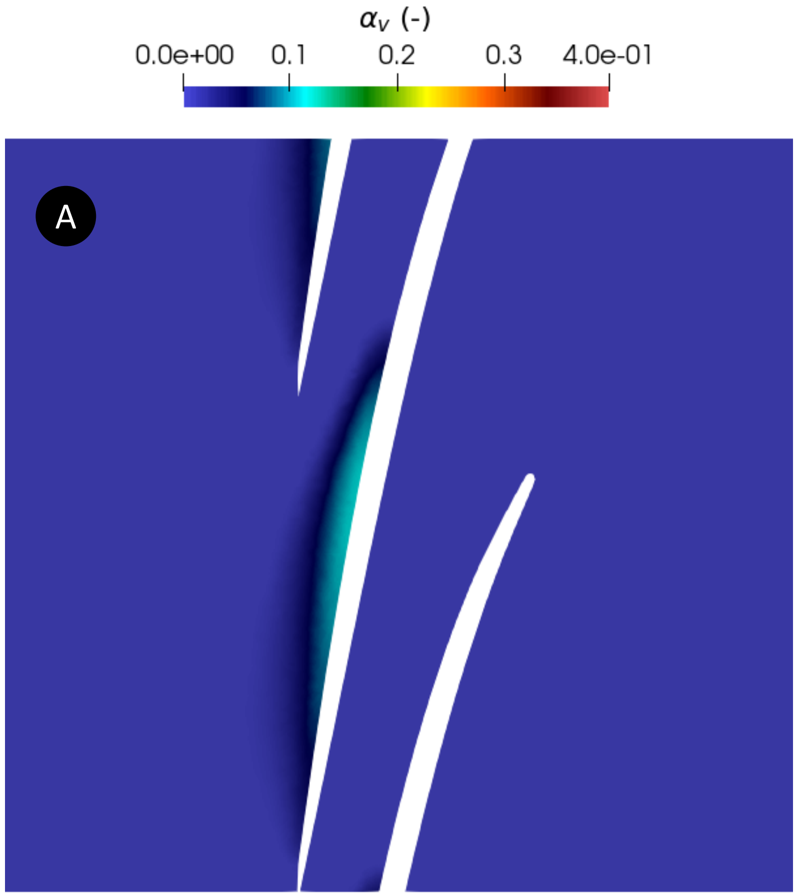

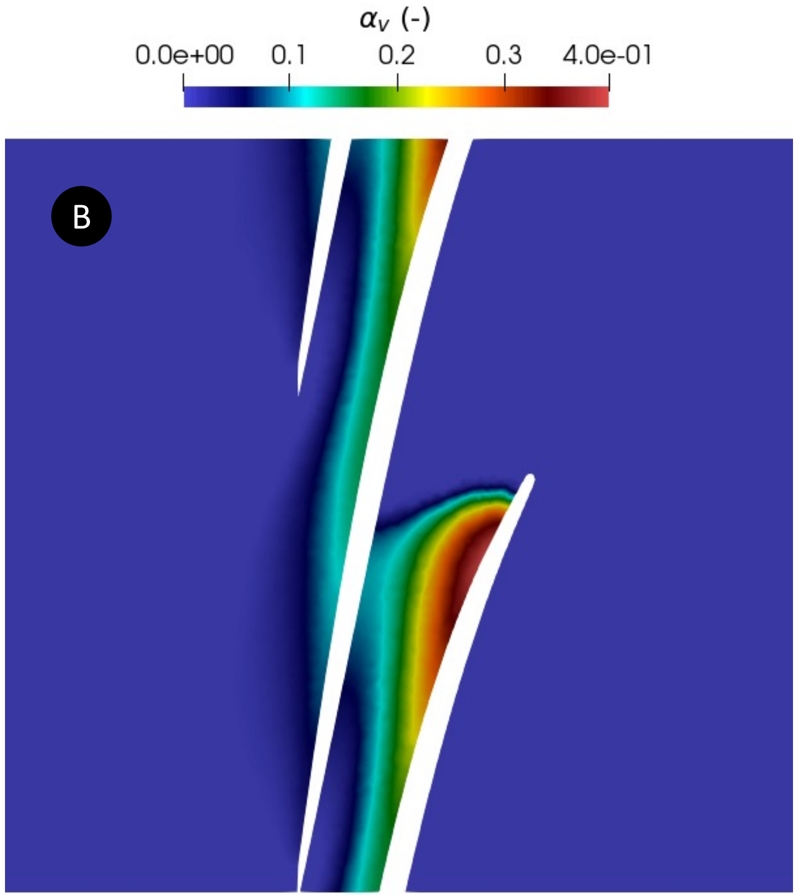

Results: two-phase flow in cavitating regime

Blades load with/without cavitation

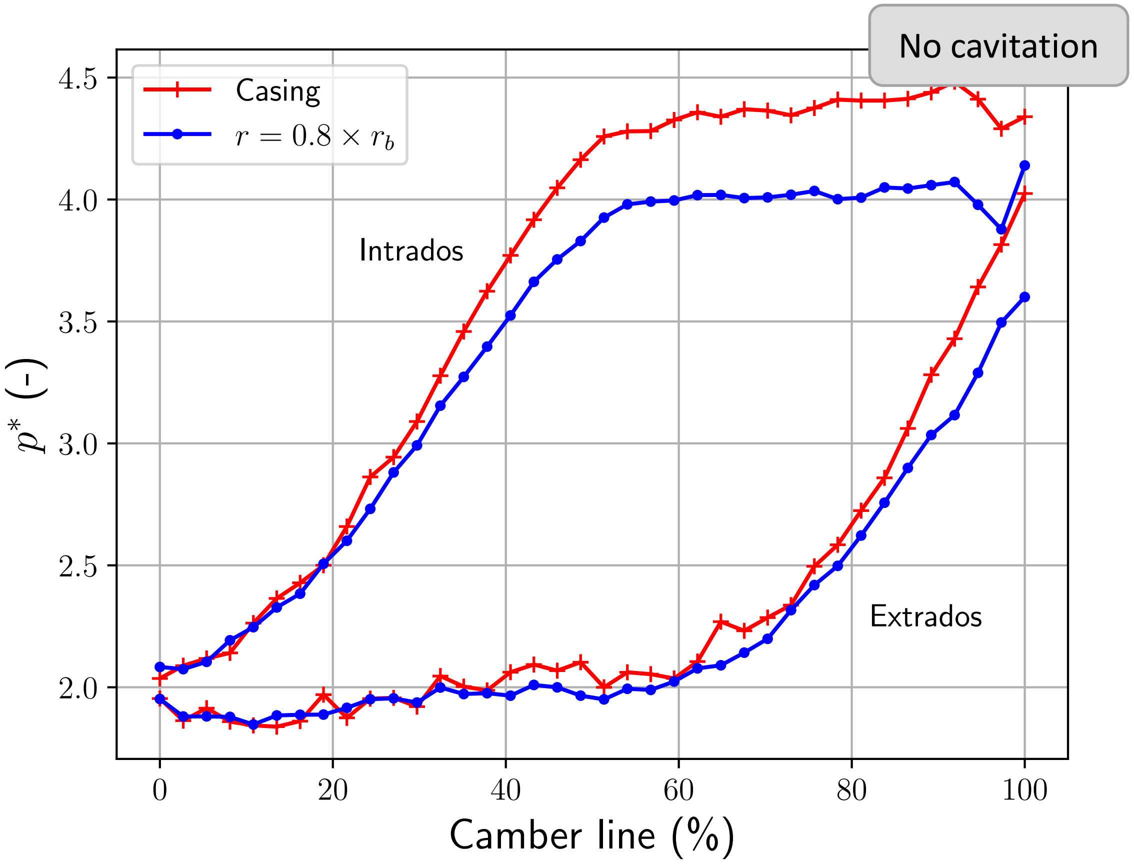

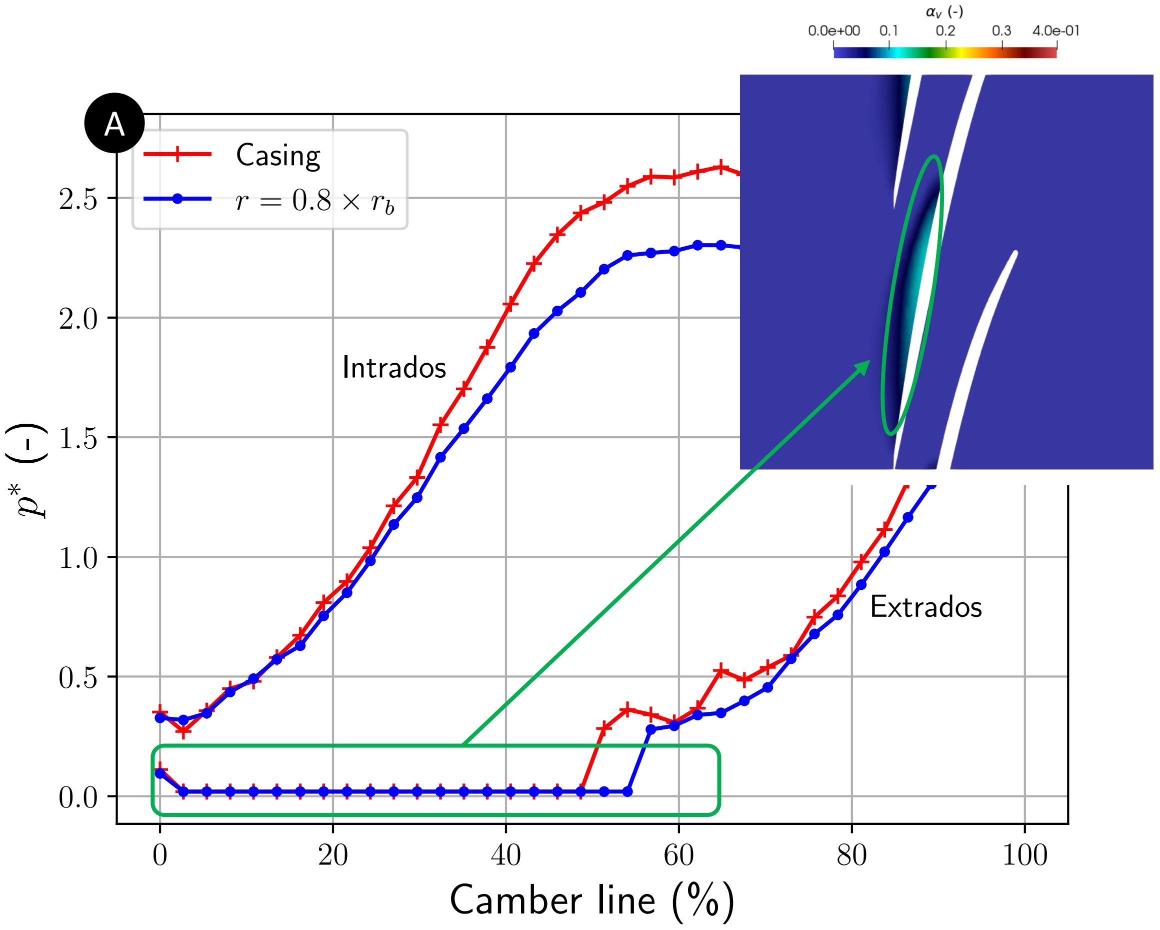

Results: two-phase flow in cavitating regime

Blades load on two cavitation regimes

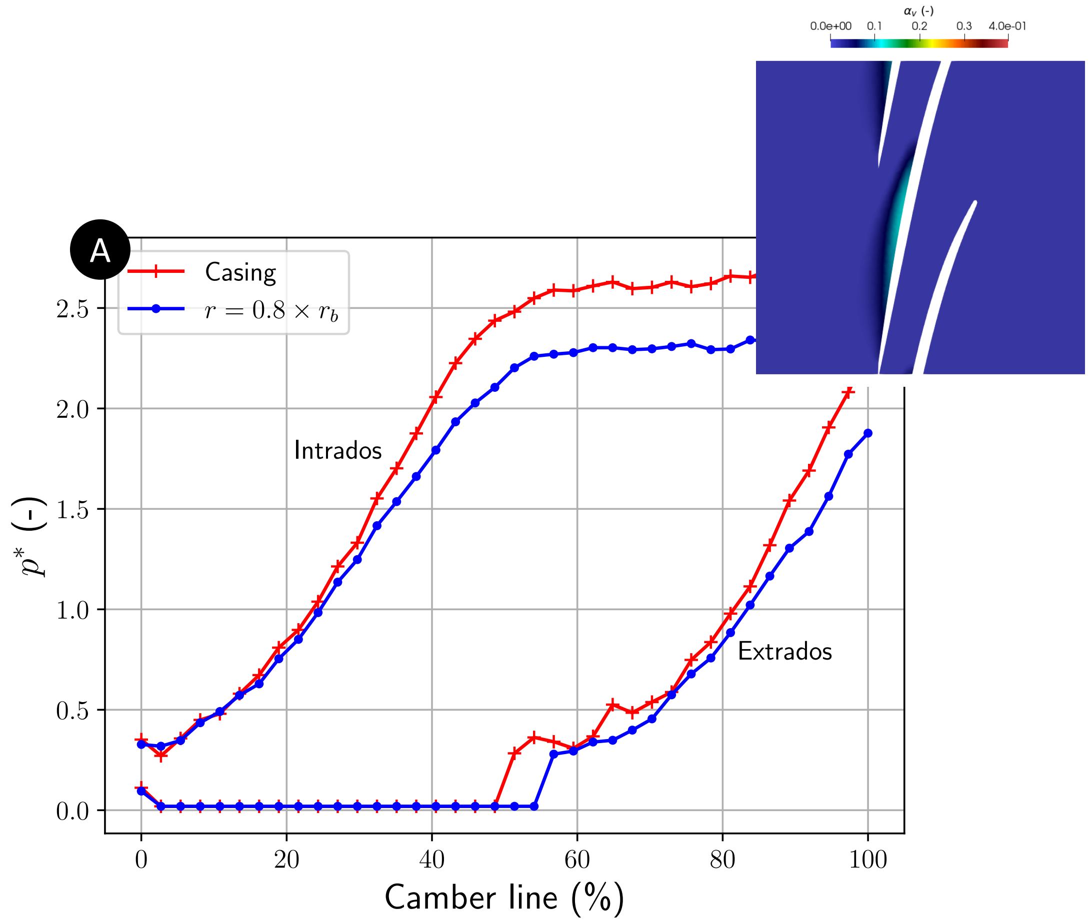

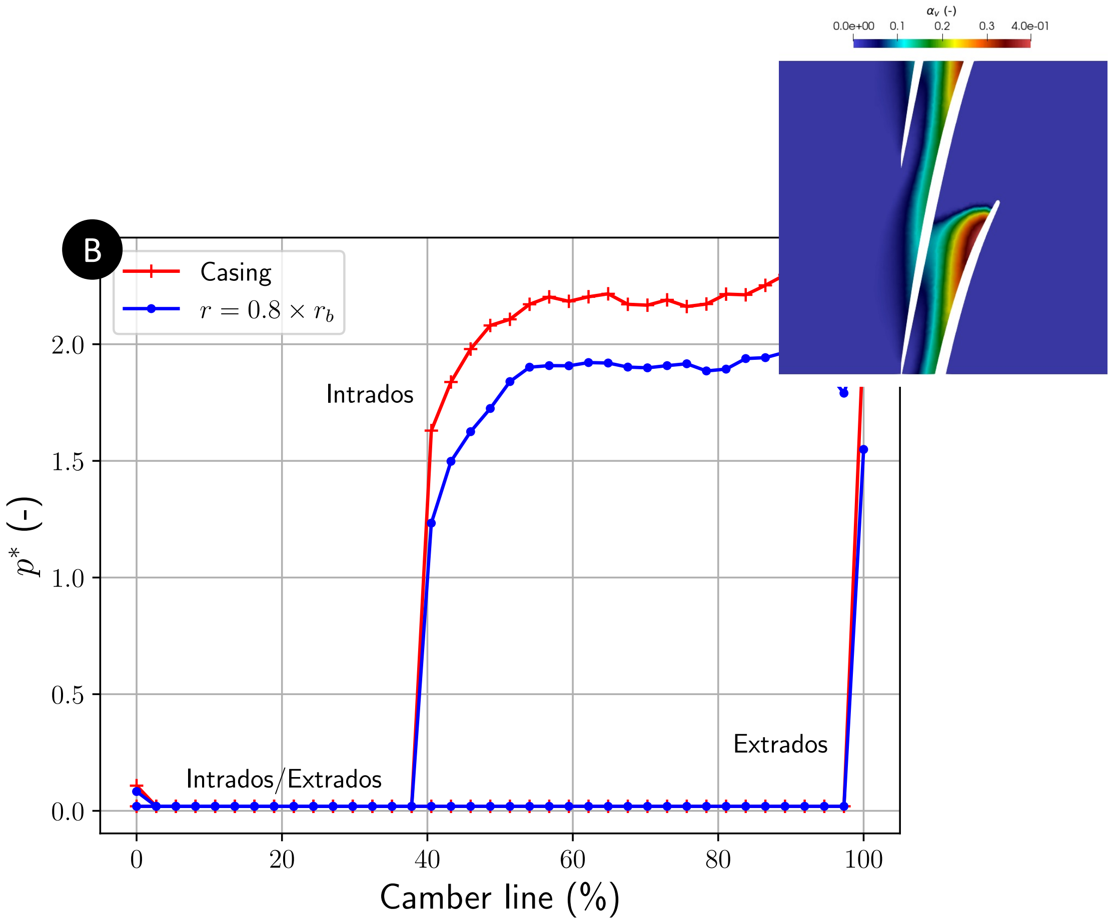

Summary

Introduction

Modeling of the cavitation phenomenon

- State-of-the-art
- Two-phase flow approach
- Two-phase flow model
- Blades motion

Numerical method

- Numerical scheme
- MRF fluxes
- Mesh mapping

Results

- Test case setup
- Single-phase flow behavior: pump characteristic
- Two-phase flow: cavitating regime

Conclusions & perspectives

Conclusions & perspectives

Conclusions

- Two-phase flow model written in a rotating frame
- Phase change based on thermodynamics
- Good estimation of an inducer behavior in non-cavitating regime
- Assessment of the performance breakdown in cavitating regime

↓

Two-phase flow model able to capture cavitation pockets in turbopumps

Perspectives

- Improve performance breakdown
  - Gap between the casing and the blades?
  - Flow temperature?
  - 2^{nd} order numerical scheme?
  - Low-Mach preconditionning?
  - Turbulence?
- Study of the thermodynamic effect responsible of a delay on the cavitation phenomenon

References

[Franz *et al.*, 1989] Franz, R., Acosta, A. J., Brennen, C. E., & Caughey, T. K. (1989)
The rotordynamic forces on a centrifugal pump impeller in the presence of cavitation.

[Braisted, 1980] Braisted D. M. (1980)
Cavitation induced instabilities associated with turbomachines.
California Institute of Technology press.

[Franc and Michel, 1995] J-P. Franc and J-M. Michel (1995)
La cavitation : mécanismes physiques et aspects industriels.
Presses universitaires de Grenoble.

[Coutier-Delgosha *et al.*, 2005] Coutier-Delgosha, O., Morel, P., Fortes-Patella, R., & Reboud, J. L. (2005)
Numerical simulation of turbopump inducer cavitating behavior.
International Journal of Rotating Machinery, *2005*(2), 135-142.

[Goncalves *et al.*, 2010] Goncalves, E., Fortes Patella, R., Rolland, J., Pouffary, B., & Challier, G. (2010)
Thermodynamic effect on a cavitating inducer in liquid hydrogen
Journal of fluids engineering 132.11

[Singhal *et al.*, 2002] Singhal, A. K., Athavale, M. M., Li, H., & Jiang, Y. (2002)
Mathematical basis and validation of the full cavitation model.
J. Fluids Eng., *124*(3), 617-624.

[Zhang *et al.*, 2019] Zhang, Y., Ren, X., Wang, Y., Li, X., Ito, Y., & Gu, C. (2019)
Investigation of the cavitation model in an inducer for water and liquid nitrogen.
Proceedings of the Institution of Mechanical Engineers, Part C: Journal of Mechanical Engineering Science, *233*(19-20), 6939-6952.

[Baer and Nunziato, 1986] Baer, M. and Nunziato, J. (1986)
A two-phase mixture theory for the deflagration-to-detonation transition in reactive granular materials.
International journal of multiphase flow, 12(6) :861–889.

[Kapila *et al.*, 2000] Kapila, A. K., Menikoff, R., Bdzil, J. B., Son, S. F., & Stewart, D. S. (2000).
Two-phase modeling of ddt in granular materials: Reduced equations.
Technical Report, LA-UR-99-3329, Los Alamos National Laboratory, USA.

[Saurel *et al.*, 2009] Saurel, R., Petitpas, F., and Berry, R. A. (2009)
Simple and efficient relaxation methods for interfaces separating compressible fluids, cavitating flows and shocks in multiphase mixtures.
Journal of Computational Physics, 228(5) :1678–1712.

[Petitpas *et al.*, 2011] Petitpas, F., Saurel, R., Ahn, B. K., & Ko, S. (2011).
Modelling cavitating flow around underwater missiles. *International Journal of Naval Architecture and Ocean Engineering*, *3*(4), 263-273.

[Le Métayer *et al.*, 2004] Le Métayer, O., Massoni, J., Saurel, R. (2004)
Elaboration des lois d'état d'un liquide et de sa vapeur pour les modèle d'écoulements diphasiques.
International journal of thermal sciences 43.3, p. 265-276.

[Le Métayer *et al.*, 2016] Le Métayer, O., & Saurel, R. (2016).
The Noble-Abel stiffened-gas equation of state.
Physics of Fluids, *28*(4), 046102.

[Combrinck and Dala, 2014] Combrinck, M., and Dala, L. (2014)
Eulerian derivations of non-inertial navier-stokes equations
29th Congr. Int. Counc. Aeronaut. Sci, 577.

[Cazé et al., 2022] Cazé, J., Petitpas, F., Daniel, E., Le Martelot, S., Queguineur, M. (2022).
Modeling and simulation of a turbopump flow: a multiphase approach.
ASME Turbo Expo 2022 - Turbomachinery Technical Conference and Exposition, Rotterdam.

[Schmidmayer *et al.*, 2020] Schmidmayer, K., Petitpas, F., Le Martelot, S., Daniel, E. (2020).
ECOGEN: An open-source tool for multiphase, compressible, multiphysics flows.
Computer Physics Communications, 251, 107093.

[Schmidmayer, Cazé *et al.*, 2022] K. Schmidmayer, J. Cazé, F. Petitpas, E. Daniel, N. Favrie (2022)
Modelling interactions between waves and diffused interfaces
International Journal of Multiphase Flow.

[Brennen, 2011] Brennen, C. E. (2011).
Hydrodynamics of pumps.
Cambridge University Press.

[Chivers, 1969] Chivers, T. C. (1969).
First Paper: Temperature Effects on Cavitation in a Centrifugal Pump: Theory and Experiment.
Proceedings of the Institution of Mechanical Engineers, 184(1), 37-47.

Thank you for your attention

Thermodynamic effect

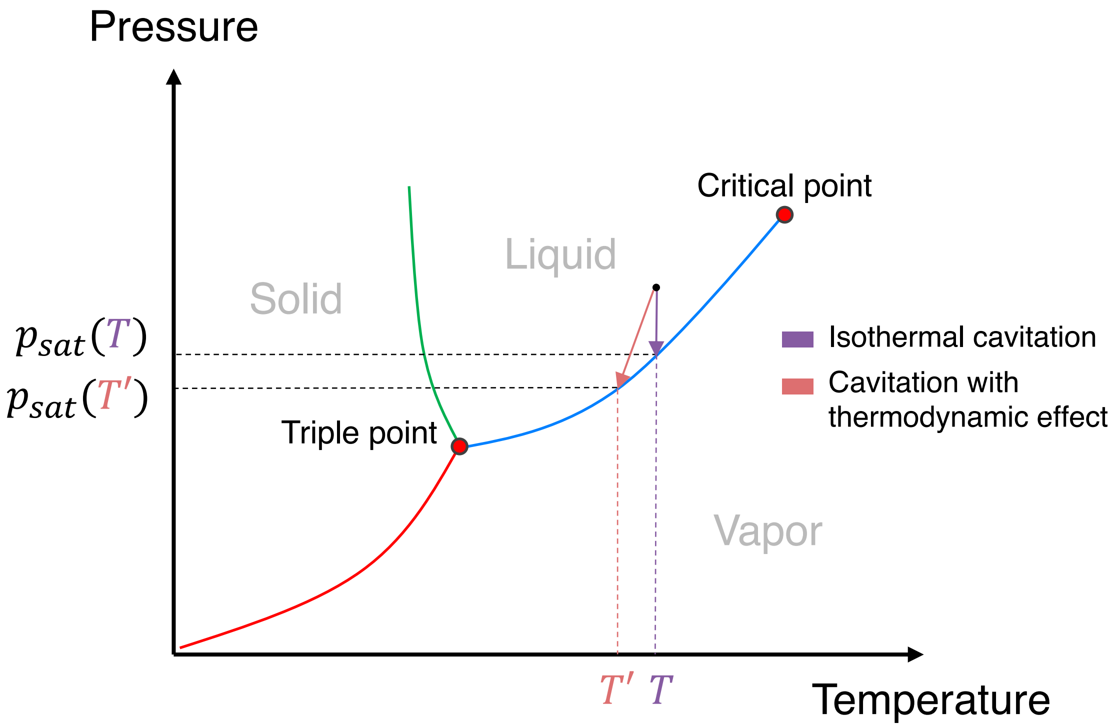

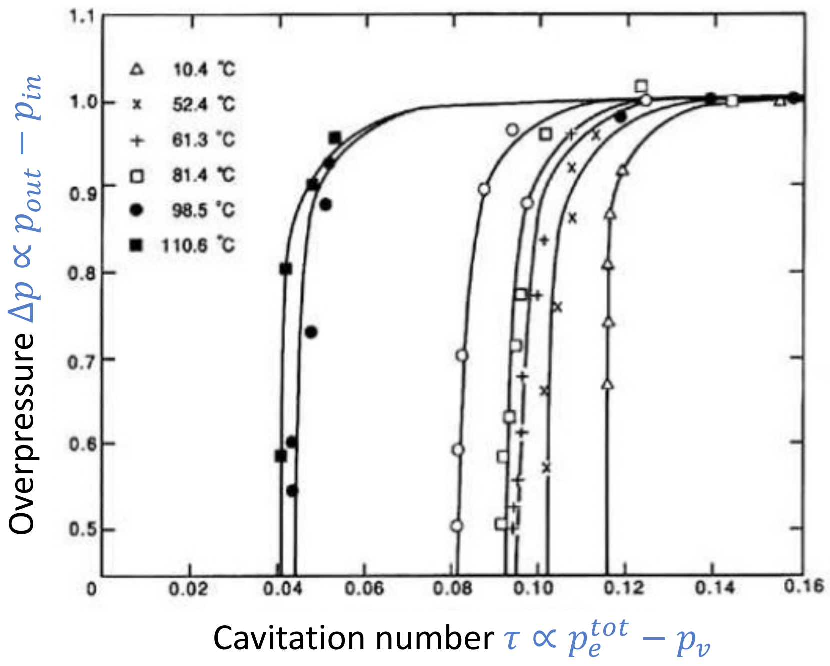

Fig – Performance curve of a water centrifugal pump [Chivers, 1969]

Two-phase flow model based on total energy equations

Internal energy formulation

$$\partial_t \alpha_1 + \nabla \cdot (\alpha_1 u) - \alpha_1 \nabla \cdot u = \mu(p_1 - p_2)$$

$$\partial_t(\alpha_k \rho_k) + \nabla \cdot (\alpha_k \rho_k \boldsymbol{u}) = 0$$

$$\partial_t(\rho \boldsymbol{u}) + \nabla \cdot (\rho \boldsymbol{u} \otimes \boldsymbol{u}) + \nabla(\alpha_1 p_1 + \alpha_2 p_2) = \boldsymbol{0}$$

$$\boxed{\begin{aligned} \partial_t(\alpha_1 \rho_1 e_1) + \nabla \cdot (\alpha_1 \rho_1 e_1 \boldsymbol{u}) + \alpha_1 p_1 \nabla \cdot \boldsymbol{u} &= -\mu p_I (p_1 - p_2) \\ \partial_t(\alpha_2 \rho_2 e_2) + \nabla \cdot (\alpha_2 \rho_2 e_2 \boldsymbol{u}) + \alpha_2 p_2 \nabla \cdot \boldsymbol{u} &= +\mu p_I (p_1 - p_2) \end{aligned}}$$

Total energy formulation

$$\partial_t(\alpha_1 \rho_1 E_1) + \nabla \cdot (\alpha_1 \rho_1 E_1 \boldsymbol{u} + \alpha_1 p_1 \boldsymbol{u}) \boxed{+ \Sigma(\boldsymbol{U}, \nabla \boldsymbol{U})} = -\mu p_I (p_1 - p_2)$$
$$\partial_t(\alpha_2 \rho_2 E_2) + \nabla \cdot (\alpha_2 \rho_2 E_2 \boldsymbol{u} + \alpha_2 p_2 \boldsymbol{u}) \boxed{- \Sigma(\boldsymbol{U}, \nabla \boldsymbol{U})} = +\mu p_I (p_1 - p_2)$$

Total mixture energy conservation

[Pelanti and Shyue, 2014]

Moving Reference Frame method